Tamaki, K., Pisciotto, K., Allan, J., et al., 1990
Proceedings of the Ocean Drilling Program, Initial Reports, Vol. 127

1. BACKGROUND, OBJECTIVES, AND PRINCIPAL RESULTS, ODP LEG 127, JAPAN SEA[1]

Shipboard Scientific Party[2]

INTRODUCTION

Leg 127 of the Ocean Drilling Program accomplished the first successful penetration of the volcanic rocks which underlie the deep basins of the Japan Sea. The basaltic rocks recovered at three of the four drilling sites provide valuable new constraints on the style and timing of volcanism and, by inference, on the origin of these basinal areas (Fig. 1). In addition, this drilling effort marks the first recovery of complete sedimentary sequences in this marginal sea. The vertical and lateral progressions of the sedimentary facies within these sequences provide the most updated view of how this marginal sea developed, from inception to the present day. Lastly, the Leg 127 drilling results unequivocally date the uplift of Okushiri Ridge and provide a minimum estimate of the initiation of compression along a zone of possible incipient subduction in the eastern Japan Sea. This active zone has been the site of large magnitude earthquakes for the past 20 yr.

In this chapter, we provide information regarding the background and objectives of this drilling expedition as well as a comparative summary of the key findings at all the sites. More extensive and specific coverages of each site are in the ensuing chapters. Leg 127 was the first of two scientific drilling ventures conducted by the Ocean Drilling Program in the Japan Sea during the summer and fall of 1989. Our drilling sites were mostly in basinal areas. In contrast, the succeeding drilling effort by Leg 128 focused on high-standing blocks and on geophysical experiments. Together, the drilling and geophysical results of these two cruises provide crucial new data needed for an understanding of the tectonic, sedimentological, and oceanographic development of this marginal sea. In a broader context, these findings aid greatly in our perceptions of the timing and mechanisms of formation of marginal basins in this region.

BACKGROUND

General

The back-arc basins and marginal seas of the western Pacific (Fig. 2) are the keys to understanding the processes of continental dismemberment, accretion, and growth in a convergent margin setting. These basins lie between two of the most dynamic regions of the earth's lithosphere, the subduction zones of the western Pacific and the Himalayan convergence. The interaction between these two regions is primarily responsible for the complex stress fields which shaped these basins (Jolivet et al., 1989). The proposed mechanisms for back-arc spreading and marginal sea formation include: (1) mantle diapirism spawned by shear strain heating of the upper surface of the underthrust lithosphere (Karig, 1971), by dewatering of the slab and partial melting of the overlying mantle (Karig, 1974), or by deep-seated and localized core-mantle interactions and heat transfer (Miyashiro, 1986); (2) convective flow induced in the asthenosphere by the subducting slab (Sleep and Toksöz, 1971; Andrews and Sleep, 1974; Toksöz and Bird, 1977; Toksöz and Hsui, 1978); and (3) seaward migration of the trench hinge line (Molnar and Atwater, 1978; Chase, 1978; Wu, 1978; Uyeda and Kanamori, 1979); retreat of the back-arc plate from the volcanic arc (Dewey, 1980); and intracontinental deformation such as the case of the Himalayan convergence (Tapponier et al., 1982; Jolivet, 1986; Kimura and Tamaki, 1986; Lallemand and Jolivet, 1986).

Within this context, no single process can easily account for the formation of all these western Pacific marginal basins. In fact, evidence gained thus far by drilling and geophysical investigations demonstrates that the marginal basins formed by a variety of processes, including single and multiaxial spreading and rifting of volcanic and continental arcs, changes in subduction polarity due to arc-arc and arc-continent collisions, transcurrent pull-aparts and displacement of continental borderlands, and entrapment of parts of larger ocean basins (Taylor and Karner, 1983; Jolivet et al., 1989). In each case, the data needed for unraveling the basin origin are the same, namely: (1) crustal structure; (2) magnetic anomaly patterns; (3) ages, compositions, and variability of basement rocks; (4) structural style and trends; (5) seismicity; and (6) sedimentary history.

The Japan Sea is perhaps the most studied of the marginal basins in the western Pacific region. Over the years, the area has been probed based on a variety of geophysical methods and geological samples (see summary in Tamaki, 1988). It is generally agreed that the basin formed some time in the mid-Tertiary and is floored in part by oceanic-type crust flanked by foundered and rifted continental blocks. Beyond this point, interpretations diverge and a host of theories have been proposed concerning the exact timing and mechanism of basin development (see summary in next section). Common to all these scenarios are two critical gaps in the database, namely: (1) the composition, age, and variability of the basement rocks which underlie the basinal areas of the Japan Sea; and (2) detailed documentation of the sedimentation history. These two needs can only be addressed by drilling and they provided the focus for our efforts on Leg 127.

In the following sections, we briefly summarize some of the key background information related to the Japan Sea in order to provide a perspective for our drilling results. More specific background data pertaining to each site can be found in the site chapters which follow.

Tectonics, Structure, and Age

Four major plates and several microplates and tectonic blocks converge in the area of the Japanese islands and eastern Japan Sea (Fig. 2). The Japan Sea lies on the eastern margin of the Eurasian Plate and is separated from the Philippine, Pacific, and North American plates by a complex border (Chapman and Solomon, 1976; Nakamura, 1983; Kobayashi, 1983; Savostin et al., 1983; Tamaki and Honza, 1985; Lallemand and Jolivet, 1986; Jolivet et al., 1989). To the southeast, the Nankai Trough is a subduction zone which marks the plate boundary between

[1] Tamaki, K., Pisciotto, K., Allan, J., et al., 1990. *Proc. ODP, Init. Repts.*, 127: College Station, TX (Ocean Drilling Program).

[2] Shipboard Scientific Party is as given in the list of participants preceding the contents.

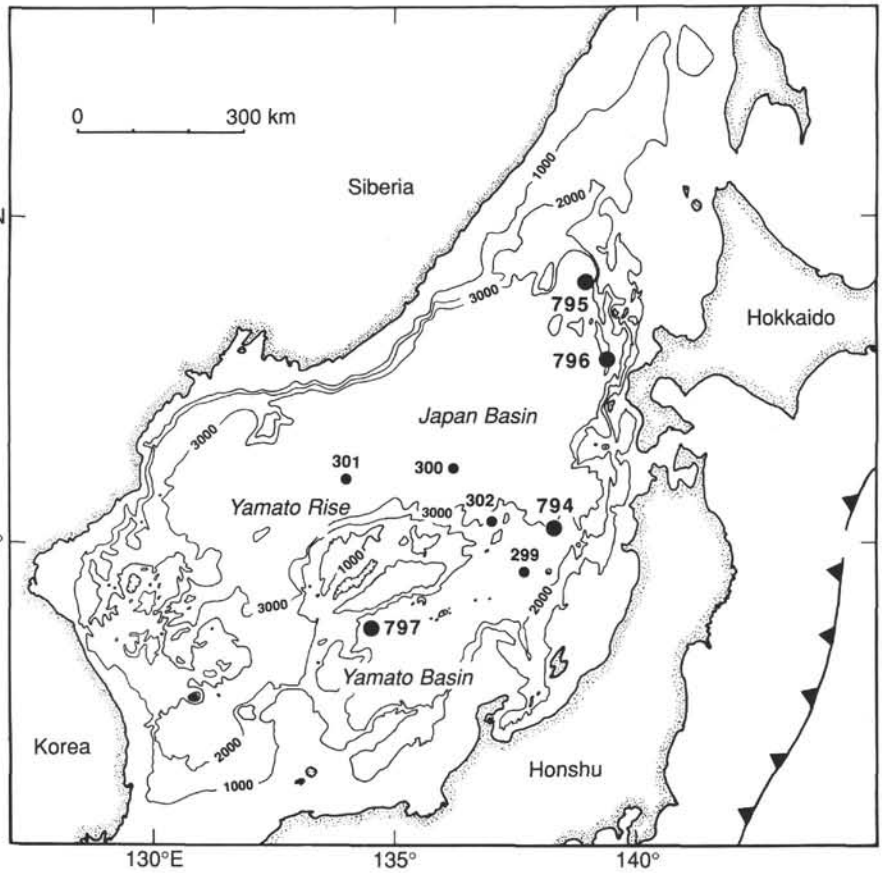

Figure 1. Map of the Japan Sea showing the locations of Leg 127 ODP Sites 794–797 and DSDP Leg 31 Sites 299–302.

the Eurasian and Philippine Plates. To the northeast the boundary bifurcates with one arm transferring to the Japan Trench, a part of the western Pacific subduction zone. The other arm runs inboard or westward of this trench, along the eastern margin of the Japan Sea, and coincides with a north-trending zone characterized by active thrust and reverse faults, large ($M > 7$) compressional earthquakes, and en-echelon seafloor ridge and basin morphology typical of transcurrent fault zones (Fukao and Furumoto, 1975; Lallemand and Jolivet, 1986; Tamaki and Honza, 1985). Although this boundary has a rather distinctive transcurrent zone morphology, the fault types and earthquake focal mechanisms and focal depths suggest that it may presently represent a young zone of incipient eastward subduction between a narrow projection of North American Plate and the Eurasian Plate (Nakamura, 1983; Kobayashi, 1983; Tamaki and Honza, 1985). If this interpretation is correct, then the eastern margin of the Japan Sea is the site of a developing plate boundary.

Patterns of faulting and the deep and shallow structure of the Japan Sea are well constrained by seismic reflection and refraction data (Ludwig et al., 1975; Gnibidenko, 1979; Tamaki, 1988; Hirata et al., 1987, 1989; Tokuyama et al., 1987; Katao, 1988). At least three structural and physiographic provinces exist and have significance for crustal structure (Fig. 3): (1) deep basinal areas, such as the Japan and Yamato Basins; (2) block-faulted ridges, typified by the Yamato Rise and Korea Rise; and (3) an eastern margin consisting of a complex of north-trending tectonic ridges and silled basins bounded by active thrust and reverse faults.

The basinal areas are characterized by a rather flat seafloor punctuated locally by seamounts. Except for these seamounts, the underlying acoustic basement is also smooth and flat, particularly in the central areas of the Yamato and Japan Basins. This character is thought to represent interbedded sediments and volcanic flows or sills which overlie a rougher basement surface (Ludwig et al., 1975; Tokuyama et al., 1987). To date, no basement samples have been recovered from these basinal areas, other than Miocene volcanic rocks dredged from the seamounts (Tamaki, 1988; Kaneoka et al., in press). As a result, the only information regarding the age and nature of the basement rocks that underlie these basins comes from these samples, and from seismic data and magnetic anomaly patterns.

The Japan Basin is the deepest and largest of the basinal areas of the Japan Sea (Fig. 3). The seafloor lies at 3.0–3.7 km and the depth to acoustic basement is 4.2–5 km below sea level (Hilde and Wageman, 1973; Ludwig et al., 1975; Tamaki, 1988). Based on refraction and gravity data, this basin is underlain by oceanic-type crust about 11–12 km thick and by a thin lithosphere which is only about 35 km thick (Fig. 4; Abe and Kanamori, 1970; Ludwig et al., 1975). In addition, the detailed marine magnetic anomaly pattern in the western part of this basin suggests complex pseudofault patterns similar to those generated by propagating spreading ridges (Tamaki and Kobayashi, 1988). Preliminary correlations with the marine magnetic anomaly time scale suggests a maximum age of about 26 Ma for this part of the basin (Fig. 5). This value is consistent with the estimates of Tamaki (1986) based on the assumption that the area is underlain by oceanic crust and using basement depth, heat flow, and stratigraphic criteria (15–30 Ma or older).

The Yamato Basin is the second prominent basin of the Japan Sea (Fig. 3). Shallower (2–2.5 km) than the Japan Basin

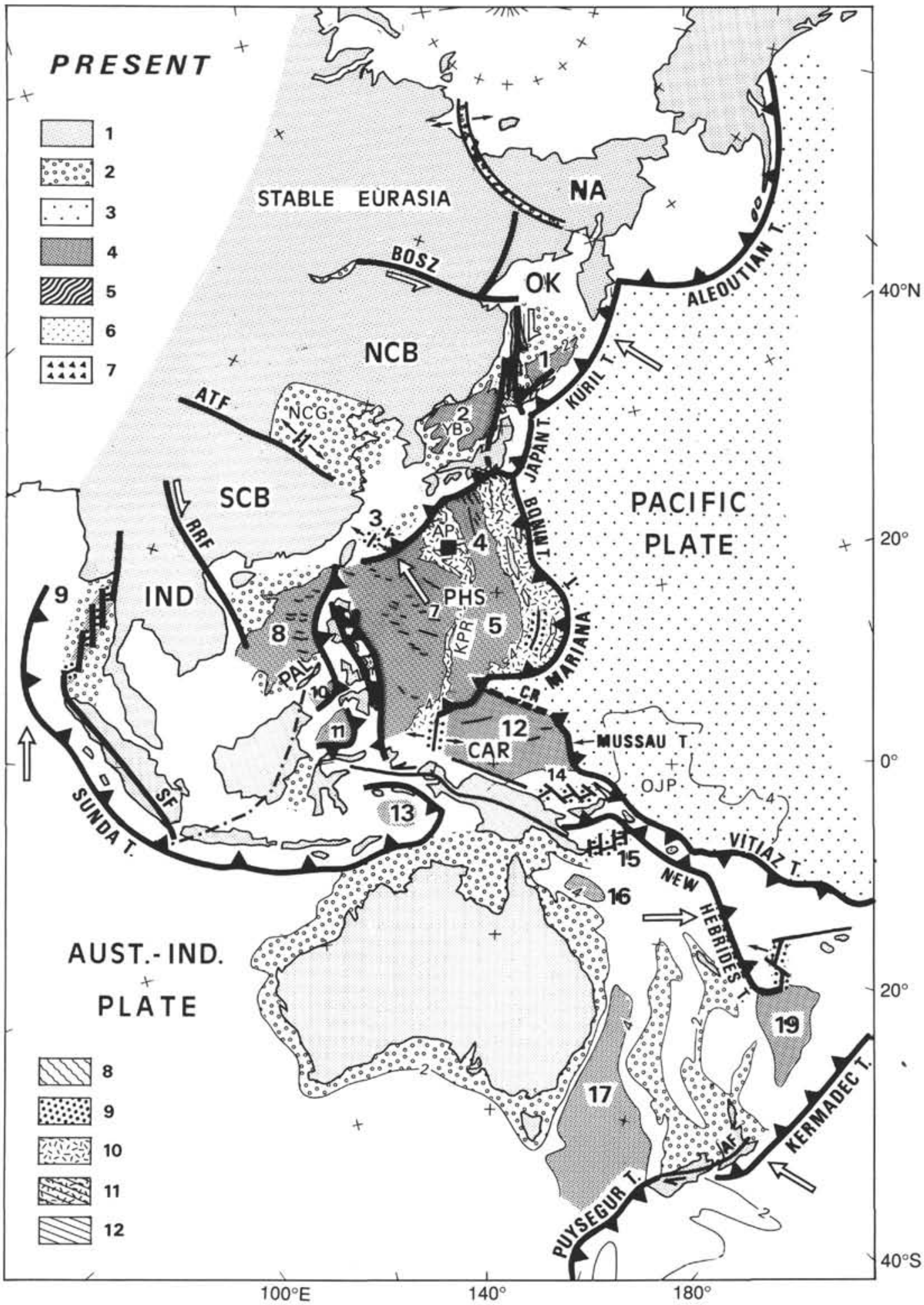

Figure 2. Tectonic map of the western Pacific region showing the positions of marginal basins in relation to the major plates and subduction zones (from Jolivet et al., 1989). Geodynamics of the Western Pacific region. Oblique Mercator projection (pole: 0°N, 50°E). 1–19: Marginal basins. 1, Kuril basin; 2, Sea of Japan; 3, Okinawa basin; 4, Shikoku basin; 5, Parece Vela basin; 6, Mariana basin; 7, West Philippine basin; 8, South China Sea; 9, Andaman Sea; 10, Sulu Sea; 11, Celebes basin; 12, Caroline basin; 13, Banda Sea; 14, Bismark rift; 15, Woodlark rift; 16, Coral Sea; 17, Tasman Sea; 18, North Fiji basin; 19, South Fiji Basin. OK, Okhotsk plate; NCB, North China block; SCB, South China block; IND, Indochina block; AP, Amami plateau; KPR, Kyushu-Palau ridge; CR, North Caroline ridge; OJP, Ontong Java plateau; BOSZ, Baikal-Okhotsk shear zone; HTSZ, Hidaka-Tartary shear zone; ATF, Altyn-Tagh fault; RRF, Red River fault; SF, Sumatra fault; AF, Alpine Fault; Black square in the PHS plate is DSDP Site 445. Patterns: 1, emerged continental crust; 2, stretched continental crust; 3, Pacific plate; 4, marginal basins oceanic crust (extinct); 5, Molucca Sea oceanic crust (only on the 12 Ma stage); 6, marginal basins oceanic crust (active spreading); 7, AUS-ANT plate oceanic crust; 8, ANT plate oceanic crust; 9, New Guinea plate oceanic crust; 10, crust of the Bonin arc and Kyushu-Palau ridge; 11, same as 10, now subducted; 12, subducted part of the Shikoku basin.

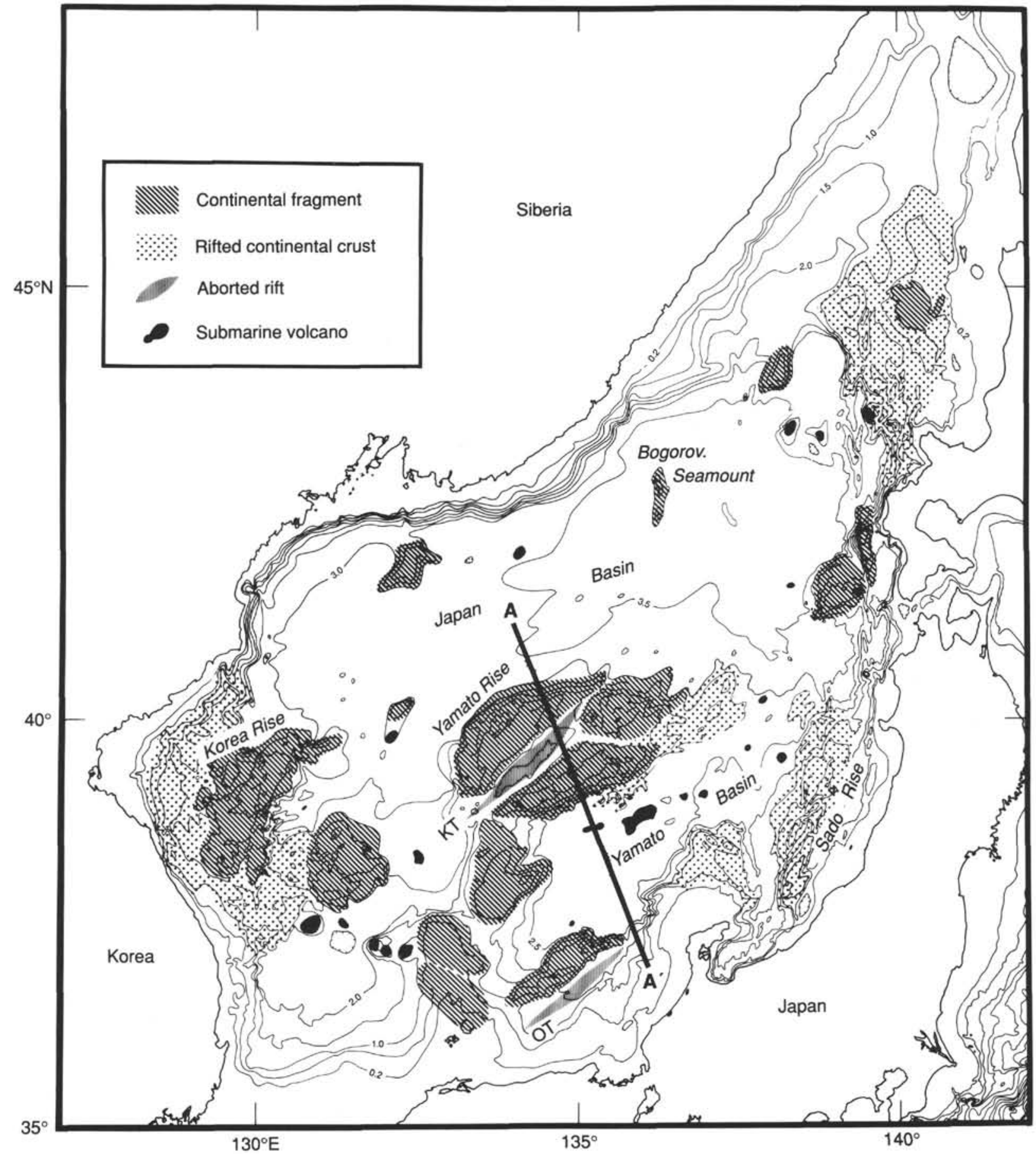

Figure 3. Map of the Japan Sea showing the geological classification of topographic highs (from Tamaki, 1988). Cross section A–A' is shown in Figure 4.

and much smaller, this basin is floored by relatively flat acoustic basement which lies 3.3–3.9 km below sea level. In addition, the crust is much thicker (17–19 km) and laterally more variable than in the Japan Basin, and not typical of oceanic crust (Fig. 4). The basin shows no clear linear magnetic anomaly patterns suggestive of spreading, but instead is characterized by chaotic, high-frequency, low-amplitude anomalies more suggestive of laterally variable volcanic terranes (Fig. 5; Isezaki, 1986). Assuming oceanic crust and using basement depths, heat flow, and stratigraphic criteria, Tamaki (1986) suggested a rather broad and uncertain age range for this basin of 15 Ma (possibly as young as 10 Ma) to 30 Ma (or older).

The high-standing blocks scattered throughout the Japan Sea comprise foundered and rifted continental fragments which are underpinned by granitic and volcanic basement rocks (Fig. 3). The Yamato Rise is the most prominent of these basement highs. It consists of two main, flat-topped and block-faulted banks separated by a narrow, partially-filled rift. The faults are principally normal faults with vertical offsets up to 1500 m. Based on the age and deformation of the overlying sediments, these faults

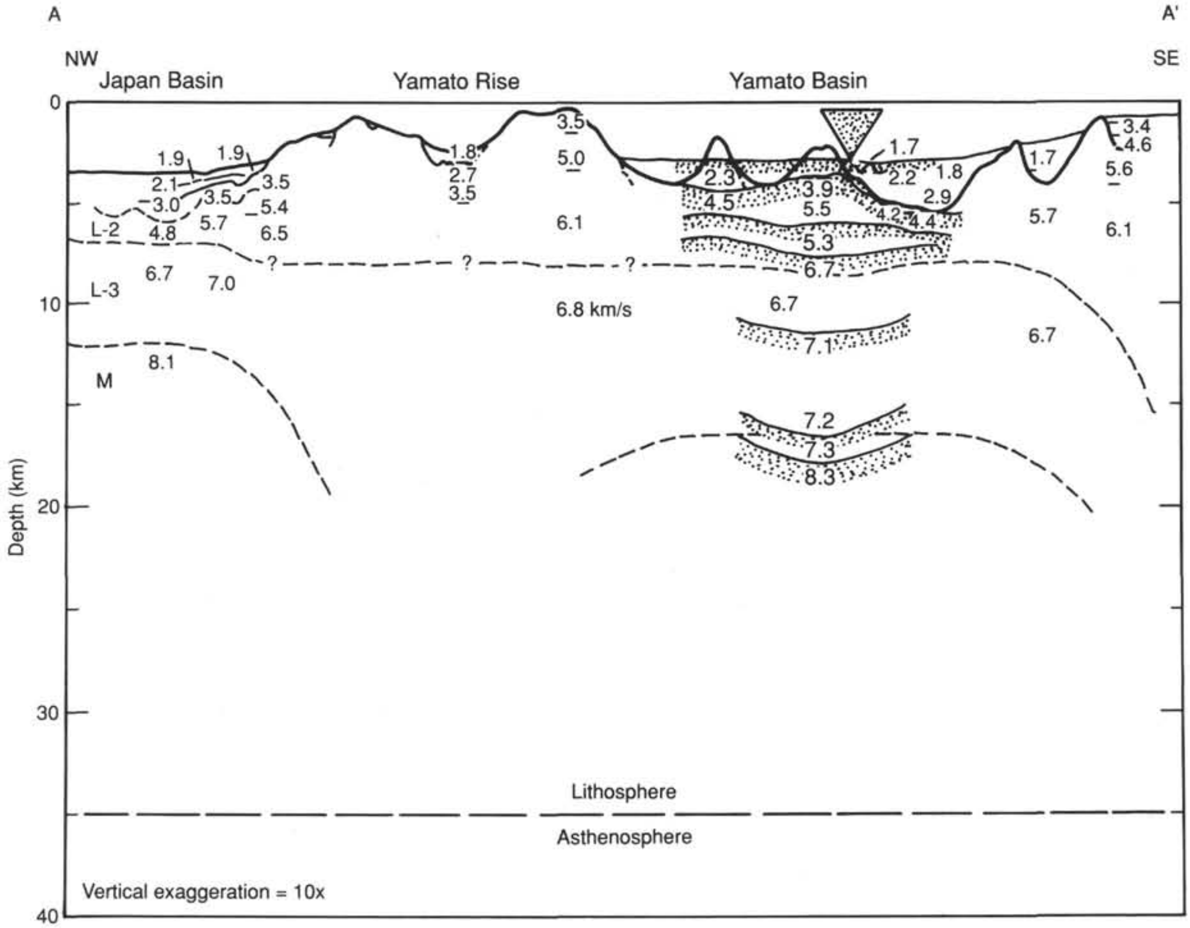

Figure 4. Crustal cross section through the Yamato Basin, Yamato Rise, and Japan Basin (from Ludwig et al., 1975; stippled segments are from Hirata et al., 1987, and Hirata et al., 1989). See Figure 3 for location.

were probably active prior to 10 Ma. Dredge samples from this area have recovered 200 Ma granitic rocks from the northwestern bank and upper Oligocene-Miocene volcanic rocks from the southern one (Kaneoka, 1986; Tamaki, 1988). No clear magnetic anomaly patterns characterize this high, and refraction data suggest that crust underneath it is at least 20 km thick (Figs. 4 and 6). The banks and shallow borderlands to the south and southwest of this rise are structurally similar and also constructed of older continental basement (Fig. 3). Mesozoic granitic rocks (60–142 Ma) prevail on these topographic highs, although Precambrian gneisses (1980–2730 Ma) have been recovered from the Korea Plateau (Tamaki, 1988).

As noted above, a north-trending complex of linear, en-echelon and fault-bounded ridges and silled basins characterizes the eastern margin and comprises the third principal structural and physiographic province of the Japan Sea (Fig. 7). This area is the only part of the Japan Sea with any shallow seismicity that is not associated with the subducting Pacific Plate. It is distinguished by large (M = 6.9–7.7, Richter scale), relatively shallow focus (14–33 km) earthquakes having hypocenters coincident with observed reverse or steep thrust faults (Tamaki and Honza, 1985). Nearly all the faults within this tectonic zone are of this type, but no consistent pattern of vergence is apparent. Based on seismic reflection data and focal depth estimates, these faults offset both continental and oceanic-type basement and, in some cases, extend through the entire lithosphere (Fukao and Furumoto, 1975). The latter observation constitutes the key evidence for the proposal of incipient eastward subduction in the east Japan Sea tectonic zone (Nakamura, 1983; Kobayashi, 1983).

The seafloor and subsurface morphology, inconsistent fault vergences, and regional tectonic reconstructions are the basis for suggesting that the structures and faults of the east Japan Sea tectonic zone are reactivated upper Oligocene to middle Miocene strike-slip features (Jolivet et al., 1989). This timing is consistent with the findings from detailed field studies in northwestern Japan. For example, Kimura et al. (1983) and Jolivet and Huchon (1989) have interpreted the Hokkaido Central Belt as a right-lateral shear zone that was active during Oligocene through middle Miocene time. Similarly, Suzuki (1979) showed that northeast-trending basins developed along the margin of northwestern Honshu during the middle Miocene and have been recently reactivated. Sugi et al. (1983) and Iijima et al. (1988) also demonstrated that the major phase of subsidence and active rifting of the northeastern Japan arc occurred during the early and middle Miocene, and additional tectonic studies on land confirm that the direction of principal horizontal compression was northeast-southwest during this period (Otsuki, 1989; Amano and Sato, 1989).

The various tectonic scenarios proposed for the development of the Japan Sea generally consider the basin to have formed by multiaxial back-arc spreading and rifting of a continental arc, ultimately reflecting the complex interactions of the Pacific, Eurasian, North American, and Philippine Plates during the past 30 m.y, perhaps longer (Tamaki, 1985; Jolivet et al., 1989).

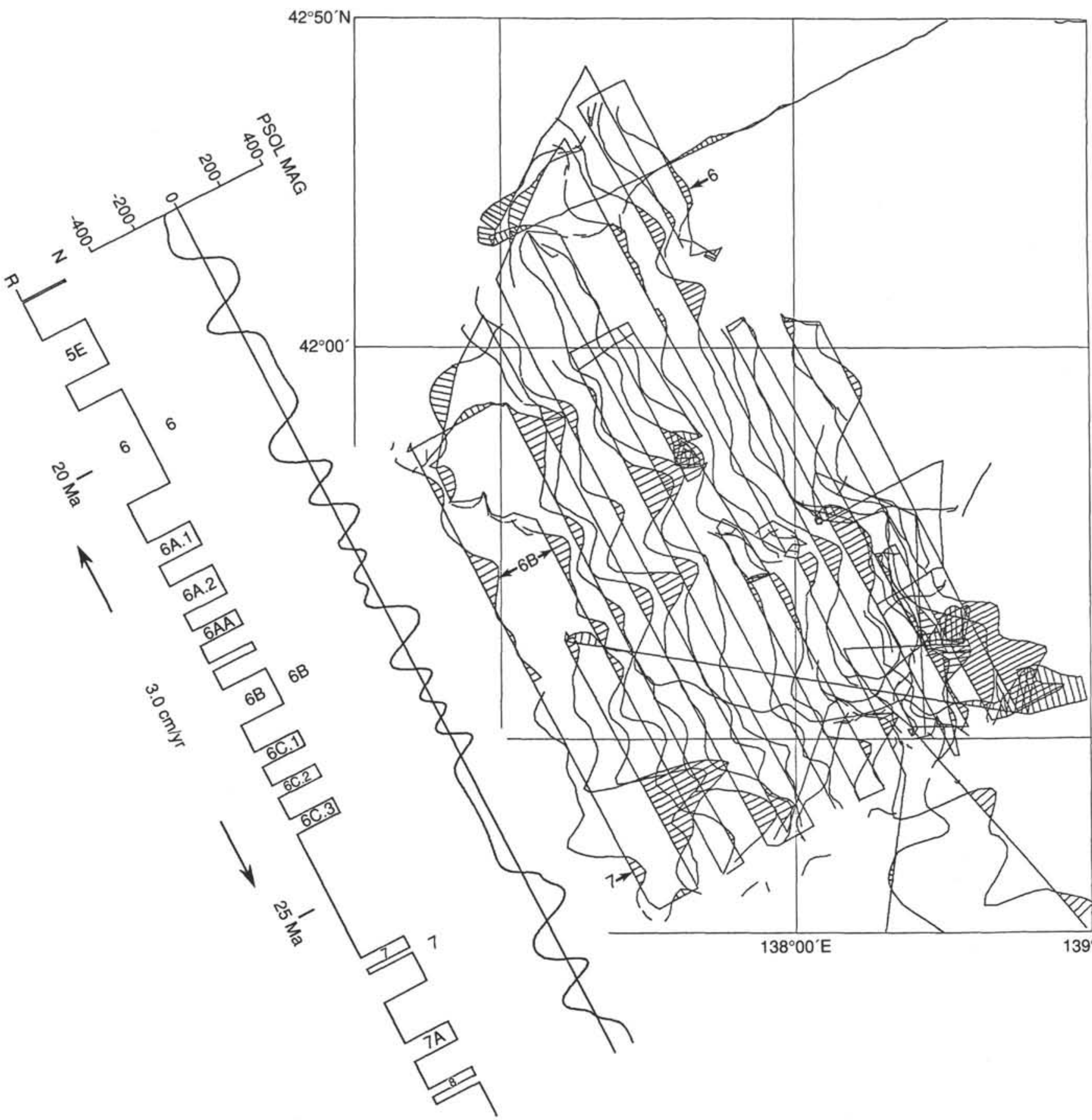

Figure 5. Detailed magnetic survey profiles in the eastern Japan Basin showing the correlation with the marine magnetic anomaly time scale (from Tamaki and Kobayashi, 1988).

In detail, specific models for how this was effected differ considerably. The proposed mechanisms include: (1) one-sided spreading of the Japan Basin beginning in the late Mesozoic or early Tertiary joined by normal spreading of the Yamato Basin at about 22 Ma (Hilde and Wageman, 1973); (2) a double, scissor-shaped opening during the late Oligocene-middle Miocene based on onshore paleomagnetic data, accommodating clockwise rotation of southwestern Japan and counterclockwise rotation of northeastern Japan (Otofuji and Matsuda, 1983; Otofuji et al., 1985; Celaya and McCabe, 1987; Tosha and Hamano, 1988; (3) regional trench roll-back resulting in concurrent opening of the Kuril Basin, Japan Sea, and Shikoku-Parece Vela Basin (Seno and Maruyama, 1984); (4) a pull-apart origin caused by right-lateral shear over a broad zone (Lallemand and Jolivet, 1986; Jolivet, 1986); and (5) single or multiaxial spreading and extension caused by the eastward retreat of Eurasia during Cenozoic time, ultimately related to the collision between India and Eurasia (Savostin et al., 1983; Zonenshain and Savostin, 1981; Kimura and Tamaki, 1986; Tamaki, 1988). Our selection of drilling targets on Leg 127 was meant to add key data useful in assessing these various models rather than to prove or disprove any particular one.

Sedimentary Framework

The Japan Sea is characterized by a Miocene and Pliocene hemipelagic sedimentary section which is draped over acoustic

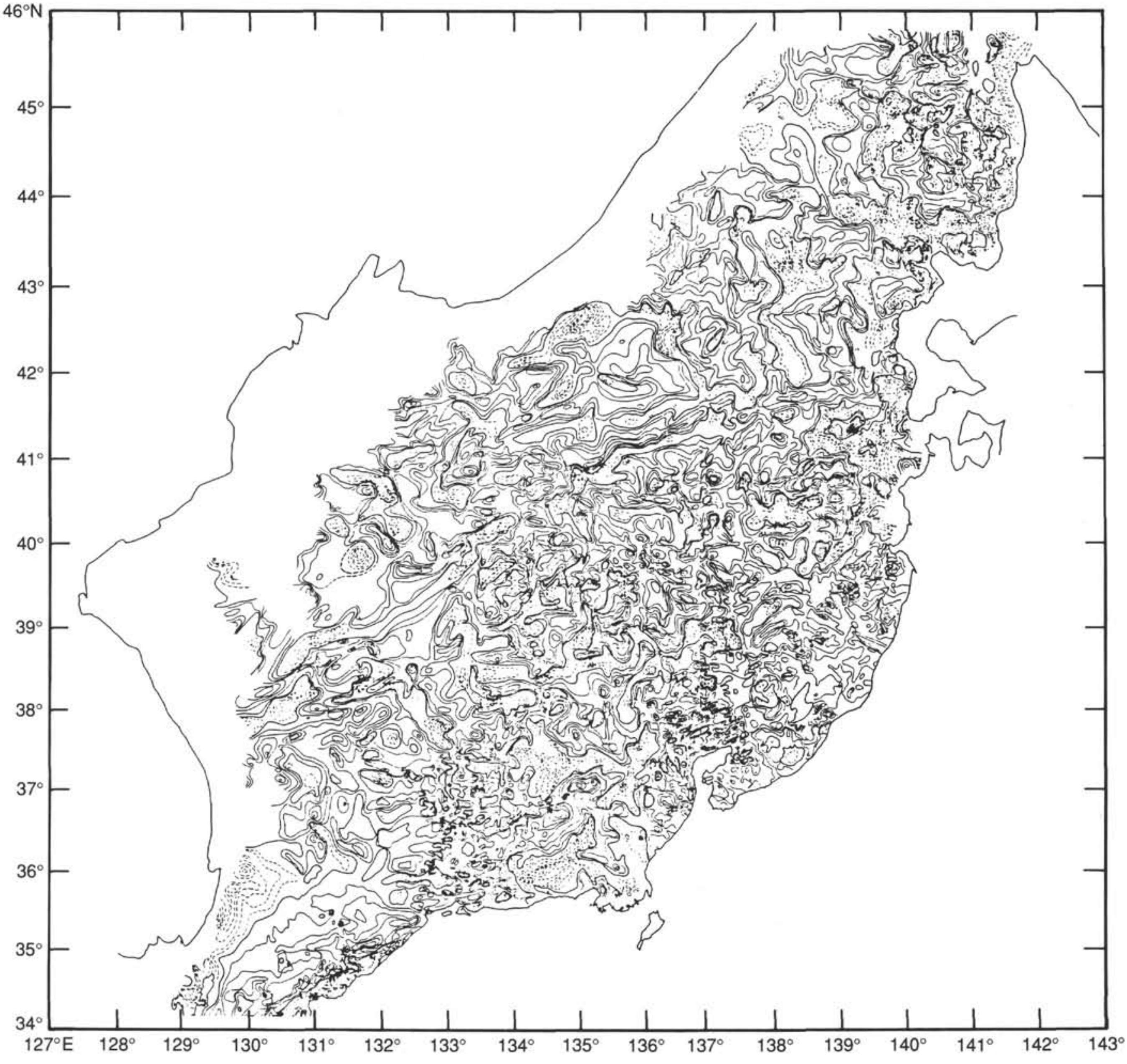

Figure 6. Map of marine magnetic anomalies in the Japan Sea (from Isezaki, 1986). The contour interval is 50 nT.

basement and is conformably and unconformably overlain by uppermost Pliocene and Quaternary hemipelagic and terrigenous sediments. The thicknesses, distributions, and character of these sediments vary directly with each of the principal structural and physiographic provinces (Fig. 8).

In the basinal areas, the sedimentary section locally reaches thicknesses of 2000–3000 m. Based on seismic data and on limited stratigraphic information available from DSDP sites and bottom samples, the section consists of two principal divisions. The upper interval is moderately well-stratified and reflective, and is composed of interbedded clays, silts, and sands of late Pliocene and Quaternary age. In some areas, these sediments comprise submarine fan deposits and are characterized by distinctive morphologic features such as incised, meandering channels and pronounced levees. The Toyama channel and fan system in the northeastern Yamato Basin is perhaps the best known and most conspicuous of these (Fig. 9; Hilde and Wageman, 1973; Karig, Ingle, et al., 1975; Ludwig et al., 1975; Boggs, 1984; Tokuyama et al., 1987). Underlying these sediments is a seismically transparent interval consisting of Miocene and lower Pliocene hemipelagic diatomaceous silts, clays, and siliceous claystones (Karig, 1975; Tamaki, 1988; Tokuyama et al., 1987). Both of these units thicken toward the centers of the basins, but toward the margins and highs, the upper unit typically onlaps the lower unit.

Compared to the basinal areas, the sediments which overlie acoustic basement of the Yamato Rise and other high-standing blocks vary considerably in thickness and character (Fig. 9; Tamaki, 1988). On some of the highest bank tops, little or no sediment is present. Where sedimentary sections are present, erosional channels and slumps are common. Based on DSDP results and bottom samples, middle Miocene through Quaternary deposits of terrigenous sand and gravel, hemipelagic silty clay, diatomaceous clay, and phosphatic mudrocks make up these

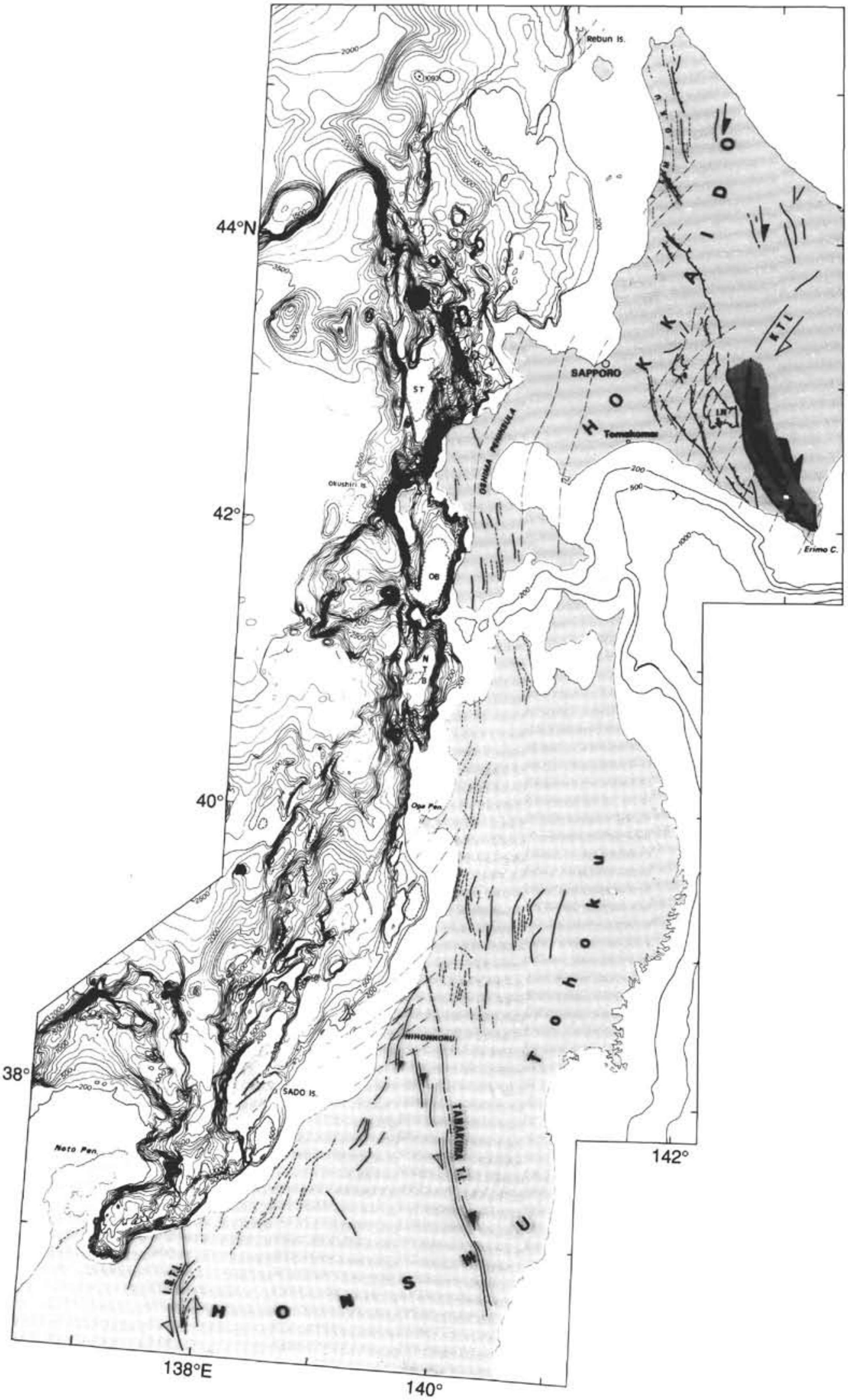

Figure 7. Map showing the detailed bathymetry of the eastern margin of the Japan Sea (from Jolivet and Huchon, 1989). Bathymetric contour interval is 100 m.

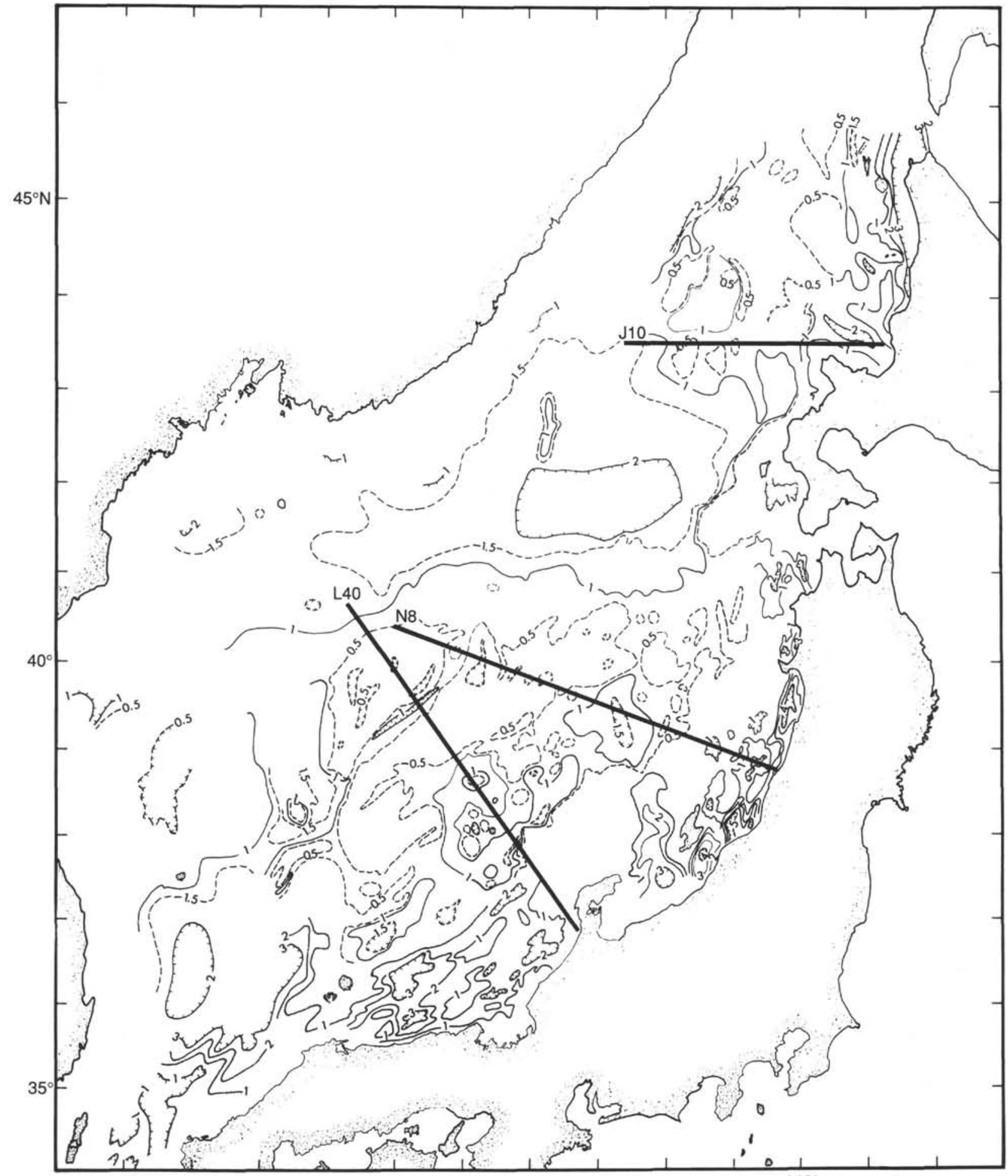

Figure 8. Sediment isopach map of the Japan Sea (from Tamaki, 1988). Contours are in seconds of two-way traveltime. Numbered lines refer to seismic lines illustrated in Figure 9.

sediments (Karig, 1975; Koizumi, 1979; Boggs, 1984; Barash, 1986). In contrast, the graben areas of these highs are often filled with considerable thicknesses (> 1000 m) of well-stratified sediments which may represent rapidly deposited and locally derived terrigenous strata interbedded with hemipelagic sediments. One of these grabens, the Kita-Yamato Trough on Yamato Rise, is a drilling target on Leg 128.

Some of the thickest accumulations of sediments occur in the small basins along the eastern margin of the Japan Sea (Fig. 8). These basins are filled with 3000–5000 m of mostly Neogene and Quaternary terrigenous and hemipelagic sediments which comprise the source and reservoir rocks for many of the oil and gas fields present along the coast of northwestern Honshu (Suzuki, 1979). Based on paleogeographic reconstructions, this re-

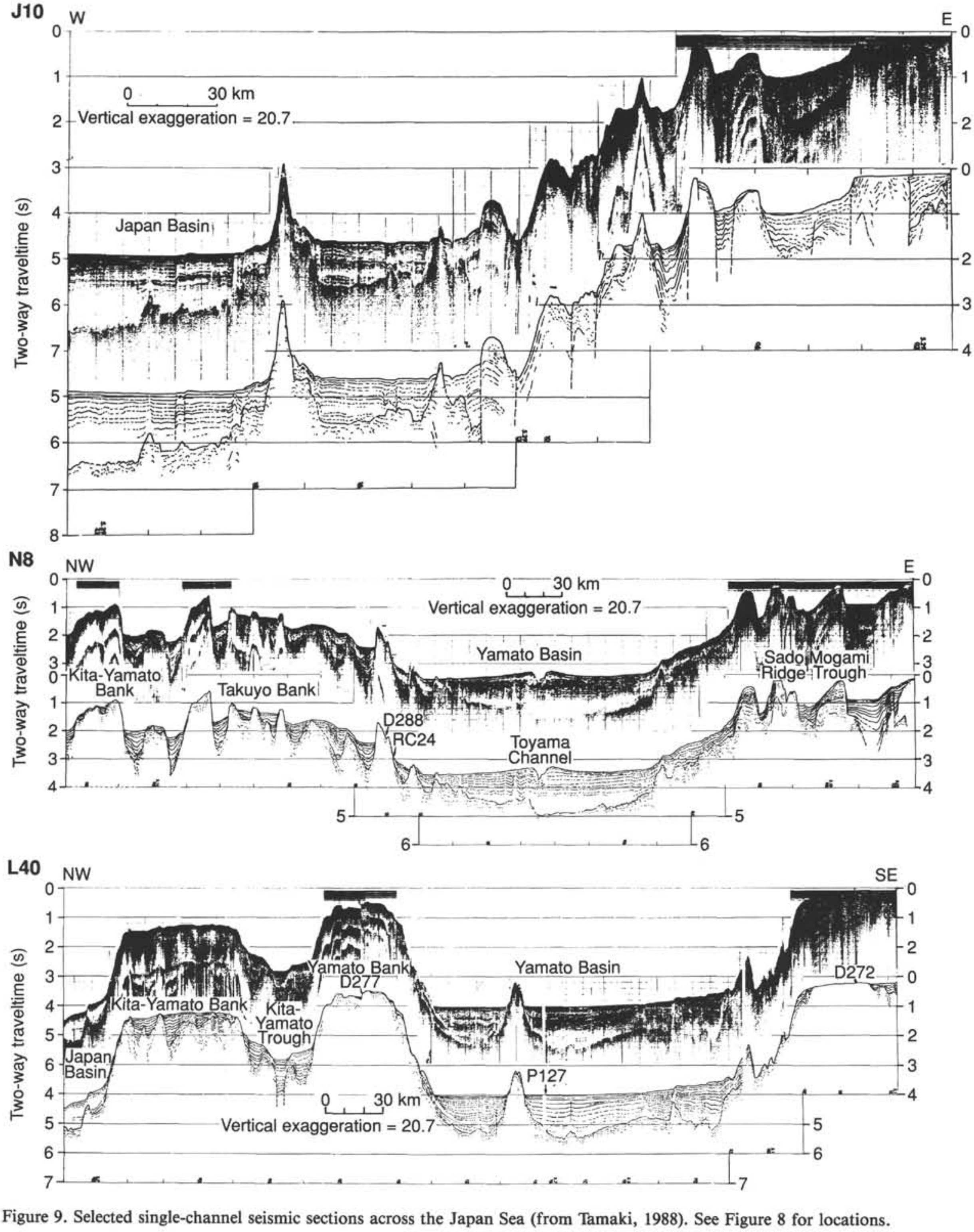

Figure 9. Selected single-channel seismic sections across the Japan Sea (from Tamaki, 1988). See Figure 8 for locations.

gion has been characterized by a complex borderland-style morphology and changeable marine conditions for the past 22 m.y. (Suzuki, 1979; Iijima et al., 1988). Many of these basins continue onshore and the sediments in them are typical of those found in many other uplifted and eroded basins of the same age on northern Honshu and Hokkaido (Fig. 10).

Many of the onshore Neogene and Quaternary deposits in Japan display a similar sequence of lithofacies, and so provide a framework for understanding the evolution of the region. When coupled with biofacies evidence of variations in paleobathymetry and paleoceanography (Asano et al., 1969; Ingle, 1975a, 1981; Koizumi, 1983, 1988; Matoba, 1984; Chinzei, 1986), recent advances in dating (Tsuchi, 1981) and offshore information from the Japan Sea (Karig, 1975; Tamaki, 1988), the lithofacies patterns collectively point to at least five phases in the late Tertiary sedimentary history of the region as outlined below.

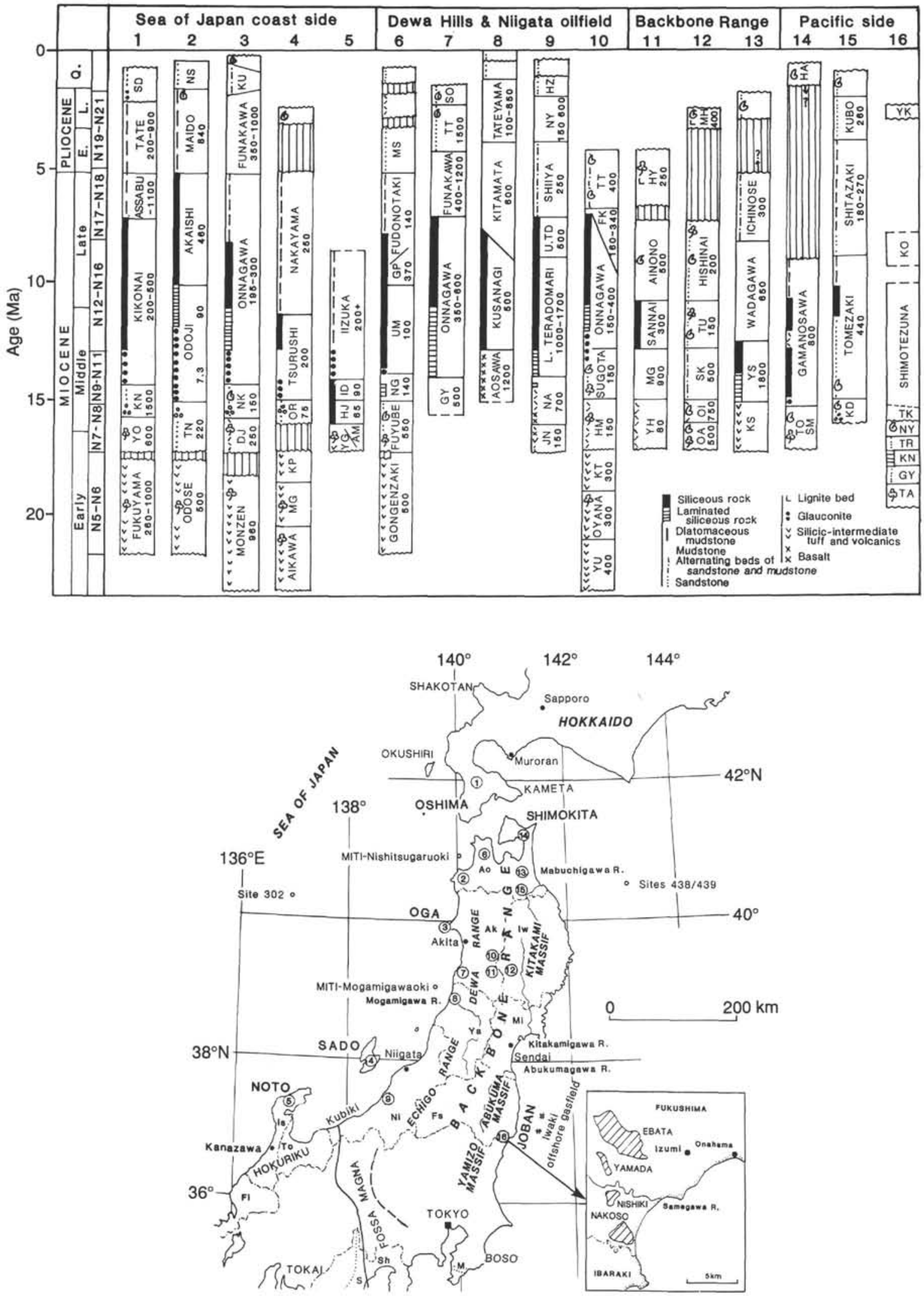

Figure 10. Index map and summary stratigraphic columns of Neogene sediments on northern Honshu (from Iijima et al., 1988).

1. *Late Oligocene-early Miocene*

This period corresponds to initial extension and rifting in the Japan Sea region coincident with widespread silicic to intermediate volcanism and deposition of pyroclastic, volcaniclastic, nonmarine, and lacustrine sediments representing the so-called "Green Tuff" unit (Takayasu et al., 1976; Koizumi, 1988; Iijima et al., 1988; Fujioka, 1986).

2. *Early middle Miocene*

During this time the volcaniclastic and nonmarine sediments of the later "Green Tuff" unit were deposited, followed by the initial deposition of marine deposits in warm water, sublittoral and neritic environments (Tsuchi, 1981; Iijima et al., 1988).

3. *Late middle and late Miocene*

Basin subsidence accelerated during this period, accompanied by pronounced climate cooling, increased rates of primary productivity, and widespread sedimentation of diatomaceous sediments at bathyal depths under oxic and suboxic water masses. Glauconitic deposits formed on isolated bank tops and large amounts of submarine basalts were extruded into intervening basins during this stage of sedimentation (Iijima et al., 1988; Tada et al., 1986)

4. *Latest Miocene and early Pliocene*

Increasing flux of terrigenous sediments occurred during this time resulting in dilution of diatomaceous hemipelagic sediments. This condition was enhanced by uplift of the northeastern Honshu arc, and the accompanying violent silicic volcanism, and by abruptly lowered sea levels in latest Miocene time which may have isolated part or all the Japan Sea behind shallow sills (Burckle and Akiba, 1978; Iijima et al., 1988; Fujioka, 1986).

5. *Late Pliocene-Recent*

This period was marked by major deposition and progradation of submarine fan systems into sub-basins and by initial, rapid filling of basins with coarse grained clastic deposits in response to compressional tectonics and uplift. Sea level fluctuations also modulated clastic input and led to episodic exclusion of Pacific Deep Water (Matoba, 1984; Iijima et all., 1988; Tamaki and Honza, 1985). The eustatic lowstands may correspond to periods of anoxic deep water, manifested in geochemically distinct sediments in the Japan Sea. The oceanographic conditions prevalent during these lowstands contrast markedly with the unusually well-mixed and entirely oxic water mass of the Holocene (Hidaka, 1966; Miyake et al., 1968; Ujiie and Ichikawa, 1973; Ingle, 1975b; Matoba, 1984).

OBJECTIVES AND STRATEGY

The principal objectives of Leg 127 were fourfold: (1) to assess the style and dynamics of rifting through determination of the age and nature of acoustic basement; (2) to characterize the sedimentation and oceanographic evolution of the region; (3) to determine the age and history of uplift and compression along the eastern margin; and (4) to measure the magnitude and direction of the present stress field. Our general strategy was formulated jointly with Leg 128. We would drill at three basinal locations in the Japan and Yamato Basins (Sites 794, 795,and 797) and one site along the eastern margin (Site 796 on Okushiri Ridge) with the principal goals noted above (Fig. 1). The objectives of Leg 128 were to drill two additional locations, both on high-standing blocks (Yamato Rise and Oki Ridge), in order to assess the oceanographic and sedimentation record which was expected to be less affected by carbonate dissolution and to investigate a possible setting for metallogenesis in a failed rift. Leg 128 also planned to revisit Site 794 in the northern Yamato Basin in order to deploy a borehole seismometer and conduct electrical resistivity experiments for crust and mantle studies.

The selection of drilling sites for Leg 127 was constrained somewhat by practical considerations. The DSDP Leg 31 drilling results told us that we would need to select basinal locations which were free from a thick section of upper Pliocene-Quaternary terrigenous sediments in order to meet our basement and paleoceanographic objectives and to avoid encountering abundant biogenic methane and possibly thermogenic hydrocarbons. Our thermal maturation models indicated that areas having no more than about 800–900 m of sediments overlying acoustic basement could be safely drilled as long as they were situated away from closures. These conditions precluded our drilling in the central areas of the Japan and Yamato Basins. In addition, data availability and political considerations dictated that we drill the marginal parts of these basins in the eastern half of the Japan Sea.

Three of the sites easily met these criteria (Sites 794, 795, and 797). The fourth site (Site 796) met all criteria except closure. This site, on Okushiri Ridge, lies within the ridge closure but was well down the flank. Our thermal models indicated that *in situ* generation of thermogenic hydrocarbons at this site was unlikely, but that we might encounter some methane and perhaps small amounts of migrated hydrocarbons (ethane).

Style and Dynamics of Back-arc Rifting

The principal goal of Leg 127 drilling in the Japan Sea was to assess the style and dynamics of back-arc rifting. In particular, our focus lay in the determination of the age and nature of the rocks comprising acoustic basement at a number of basinal localities. Previously, basement samples had been recovered only from high-standing blocks and seamounts in this marginal sea. While these rocks established the existence of volcanic terranes and foundered continental blocks, they shed little light on the nature of the basement or ages of formation of the intervening basins. In addition, we planned to recover complete sedimentary sections above basement at the drill sites in order to assess the subsidence history of the basin. Together with the new information on the age and composition of the acoustic basement, these data would provide the first direct evidence from the basinal areas for the timing and style of processes which shaped the Japan Sea.

All four sites were targeted to penetrate acoustic basement and to recover the complete overlying sedimentary section. Sites 794 and 797 were located in the Yamato Basin and Sites 795 and 796, along the eastern margin of the Japan Basin (Fig. 1). Site 796 represented a special case, where seismicity and seismic reflection data suggest that oceanic-type crust of the eastern Japan Basin is currently being obducted.

Oceanographic and Sedimentation History

A second major objective of the Leg 127 drilling was to characterize the oceanographic and sedimentation history of the Japan Sea. Sites 794, 795, and 797 were all located so as to obtain mostly hemipelagic sediments rather than terrigenous gravity flow deposits because the hemipelagic strata are more likely to contain the diagnostic microfossil assemblages needed for temporal reconstructions of climate, water mass, and subsidence. Our specific goals were: (1) to determine the history of anoxia, circulation, and sea level in relation to climate and subsidence; (2) to track the fluctuations and character of the CCD; and (3) to document the nature of time- and temperature-controlled postdepositional processes, particularly those involving organic matter, biogenic silica, and carbonate. The integration of these results with other regional onshore and offshore data would form the basis for an understanding of the sedimentation and oceanographic history of the Japan Sea in relation to the western Pacific.

Timing and Style of Compression of the Eastern Margin

A further important objective of the drilling on this leg was documentation of the timing of compressional deformation of the eastern margin of the Japan Sea. This margin is a north-trending zone characterized by active thrust and reverse faults, large compressional earthquakes, and en-echelon seafloor ridge and basin morphology. By many tectonic reconstructions, this zone represents a plate boundary in the making. As such, it records the recent tectonic history and offers a preview of the fate of this part of the Japan Sea.

Site 796 was the only site on this leg designed to investigate the timing and style of compression of the eastern margin (Fig. 1). The occurrence of shallow, datable, terrigenous sands was anticipated at this site and measurement of the magnitude and direction of the *in-situ* stress was planned. Ideally, the shallowest sand would mark the latest time that terrigenous gravity flow deposits could reach the site. After this date, uplift of Okushiri Ridge, or formation of intervening traps between the presumed eastern source and the site position, would have prevented gravity flow deposits from reaching the site. The measurement of the present stress field is considered below.

Present Stress Field

A final objective of the drilling on this Leg was an assessment of the magnitude and direction of the present horizontal stress field of the Japan Sea. To achieve this goal, we planned packer, hydrofracture, and Borehole Televiewer work at two sites (Site 794 and 796) and Borehole Televiewer runs only at the other two sites (Sites 795 and 797; Fig. 1). Given the occurrence of suitable intervals of massive and relatively unfracture basement rocks at these sites, the packer and hydrofracture experiments would measure the rock strengths and the directions of induced fractures and thus provide estimates of both magnitudes and directions of *in-situ* maximum horizontal stress. The Borehole Televiewer mainly provides information on present minimum horizontal stress directions in the form of borehole breakouts. Our strategy was to obtain complete measurements within the basement rocks at one locality within the active tectonic zone along the eastern margin of the Japan Sea (Site 796) and at an additional position in the central Yamato Basin away from this zone (Site 794). The minimum horizontal stress measurements at Sites 795 and 797 would provide comparative information. These data, in concert with similar onshore data and earthquake results, would provide the first integrated, regional view of the Japan Sea and Japanese Islands.

PRINCIPAL RESULTS

We drilled four sites on Leg 127 (Fig. 1 and Table 1) and realized nearly all of our important objectives. At Sites 794, 795, and 797 we cored lower and middle Miocene basaltic rocks comprising acoustic basement and recovered the complete sequences of overlying Neogene and Quaternary hemipelagic sediments. At Site 796 we succeeded in finding the shallow sands which precisely date the initiation of uplift of the Okushiri Ridge at 1.8 Ma. We were not able to reach acoustic basement at this site because of hole instability. Hole conditions also thwarted most of our attempts at acquiring reliable *in-situ* stress measurements. Borehole Televiewer measurements made at Sites 796 and 797 over short sedimentary and igneous intervals provided some data. In contrast, we were only able to deploy the packer at Site 797, but were unable to inflate it before the hole deteriorated. Despite these difficulties, the Leg 127 drilling was successful in attaining the important scientific goals.

The following comparative summaries present the principal results of the leg according to the subdisciplines set forth in the site chapters. These are meant to provide the specialist with a synopsis of all four sites drilled during Leg 127. A conclusions section follows which highlights the key findings as they relate to the principal objectives.

Lithostratigraphy

Approximately 2300 m of lower(?) Miocene to Quaternary marine sediment was penetrated at four sites during Leg 127 drilling in the Japan Sea. Five principal lithofacies dominate the stratigraphic sequence (Fig. 11); (A) Quaternary to Pliocene laminated, dark-colored silty clay alternating with nonlaminated, bioturbated, light-colored silty clay; (B) Pliocene to upper Miocene diatom ooze, generally bioturbated throughout; (C) middle to upper Miocene bioturbated diatom clay to faintly laminated siliceous claystone and silty claystone, with thin chert layers and minor calcareous layers and nodules; (D) middle to upper(?) Miocene calcareous and siliceous claystone and interbedded tuff with minor phosphate; and (E) lower Miocene volcaniclastic sandstones and siltstones which are graded, planar- to cross-laminated and bioturbated and are interlayered with basalts. Although widely distributed, all of these facies were not

Table 1. Coring summary for Leg 127 sites.

Hole	Latitude (N)	Longitude (E)	Water depth (m)	Total penetration (m)	Coring method	Number of cores	Cored (m)	Recovered (m)	Recovery (%)
794A	40°11.41′	138°13.86′	2810.9	351.3	APC/XCB	37	351.3	302.2	86.0
794B	40°11.40′	138°13.87′	2810.9	549.0	RCB	27	249.2	87.4	35.1
794C	40°11.40′	138°13.86′	2809.1	653.7	RCB	14	93.9	33.2	35.4
Total (794)						78	694.4	422.8	60.9
795A	40°59.23′	138°58.03′	3300.2	365.9	APC/XCB	39	364.9	258.3	70.8
795B	43°59.24′	138°57.87′	3298.9	762.2	RCB	41	397.0	188.9	47.6
Total (795)						80	761.9	447.2	58.7
796A	42°50.93′	139°24.67′	2570.6	242.9	APC/XCB	27	242.9	155.3	63.9
796B	42°50.92′	139°24.85′	2622.6	464.9	RCB	33	293.8	85.3	29.0
Total (796)						60	536.7	240.6	44.8
797A	38°36.94′	134°32.16′	2862.2	12.9	APC	1	9.5	9.7	102.4
797B	38°36.94′	134°32.16′	2862.2	495.7	APC/XCB	53	495.7	370.7	74.8
797C	38°36.93′	134°32.18′	2864.5	903.0	RCB	46	419.0	164.2	39.2
Total (797)						100	924.2	544.6	58.9
Totals						318	2917.2	1655.2	56.7

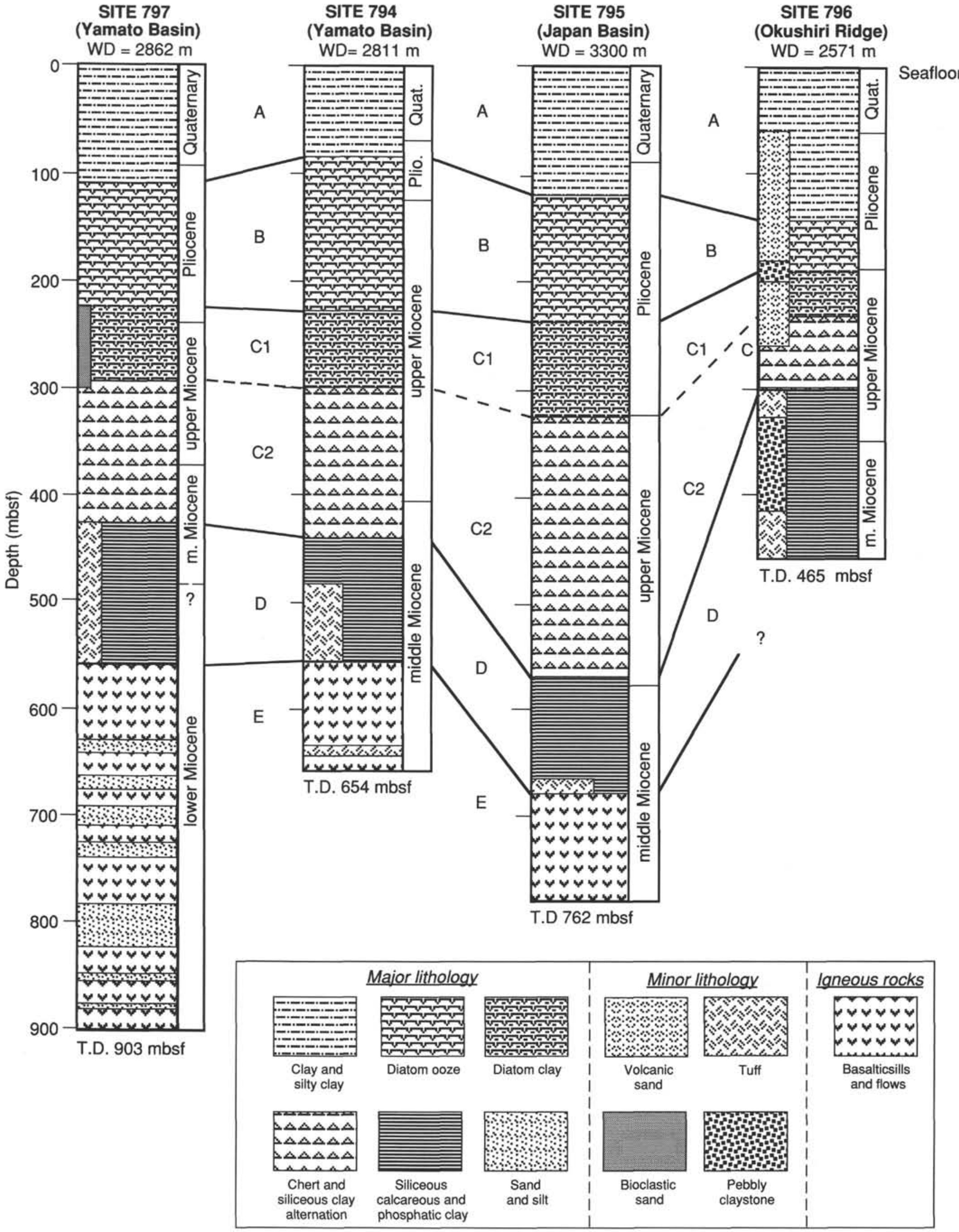

Figure 11. Summary of lithofacies encountered at Leg 127 sites. Letters A through E denote lithofacies discussed in the text.

encountered at each site. Facies E was drilled only at Sites 794 and 797 in the Yamato Basin. Facies D, identified unequivocally at Sites 794, 796, and 797, is lower Miocene in Site 797 and middle Miocene elsewhere and is, therefore, diachronous. Facies A through C occur at all sites. Two additional lithofacies occur at Site 796. The first comprises upper Miocene pebbly claystone, with minor poorly sorted, matrix-supported, pebble conglomerate containing pumice and other volcanic clasts. The other lithofacies at this site consists of Pliocene to upper Miocene fine- to medium-grained sandstone with graded bedding and parallel lamination.

The stratigraphic sequence penetrated at the Leg 127 sites suggests four main phases of deposition in the eastern Japan Sea in post-Oligocene time. Phase one occurred in early(?) Miocene to early middle Miocene time during initial development of the Yamato Basin. This phase was characterized by rapid deposition of volcaniclastic sandstones and siltstones (Lithofacies E in Fig. 11) at a basin margin in a shelf or slope setting. An abrupt increase in water depth following deposition of this sand unit is indicated by the lower middle bathyal sediments that overlie basaltic sills and flows at Site 797.

The rapid deepening of the basin, initiated during the early Miocene in the Yamato Basin and early middle Miocene to the north, marks the second phase of deposition. This phase extended from early Miocene to possibly as late as late Miocene time and was characterized by deposition of fine-grained, diatomaceous and calcareous clay-rich pelagic and hemipelagic mud and minor tuff (Lithofacies D on Fig. 11). Benthic foraminifer assemblages, the variations in degree and style of bioturbation features, and the preservation state of depositional lamination suggest alternating oxic to dysaerobic bottom-water conditions during late, early, and middle Miocene time. The absence of coarse clastic deposits other than gravity flow tuffs at Sites 794, 795, and 797 suggests that these sites were either bathymetrically isolated or too distant from major sources of terrigenous clastic input during this time. Emplacement of widespread "blue tuff" episodically throughout this period indicates significant intrabasinal explosive submarine volcanism of similar composition at widely scattered localities.

The third depositional stage is characterized by the diatomaceous and siliceous hemipelagic sediments of Lithofacies C and B during the late Miocene and Pliocene. These sediments reflect an apparent increase in diatom productivity and sedimentation. Good basin circulation and generally oxic bottom water conditions prevailed during much of this period, as indicated by diatom abundance and the presence of upwelling species, and the prevalence of bioturbation structures in most upper Miocene to Pliocene diatom oozes and claystones.

The final depositional phase extended from Pliocene to the present. This phase was dominated by sedimentation of fine hemipelagic muds (Lithofacies A) at mainly bathyal depths, punctuated by deposition of numerous thin layers of subaqueous, fallout tephra. Alternation of dark-colored, laminated silty clays and light-colored, bioturbated silty clays apparently reflects fluctuations in terrigenous input and bottom water oxygen levels during the latter half of the Quaternary. The onset of anoxic or low oxygen conditions may have been related to tectonic development of bathymetric sills and coincident sea level changes leading to basin isolation and restricted circulation. Alternatively, increased productivity in surface waters tied to climate changes and ocean circulation may have resulted in lowered oxygen levels at the sediment/water interface owing to oxidation of excess organic matter. Fluctuation in sedimentation rates may have been an additional factor that contributed to development of the distinctive light and dark color bands in the Quaternary sediments, either by episodic supply of organic matter in mud turbidites or by rapid periodic burial of organic-rich basinal sediments by gravity flow deposits. This phase also corresponds to a period of intense subaerial, explosive volcanism and uplift in the northeast Honshu arc adjacent to the Japan Sea, as documented by on-land studies. The volcanogenic sands encountered at Site 796 provide further evidence of this on-land tectonic activity. Cessation of sand deposition at Site 796 at about 1.8 Ma suggests initiation of uplift of Okushiri Ridge. These data constitute the first hard evidence for the timing of compression of this margin.

The diagenetic history of the sediments encountered at Leg 127 sites is dominated by changes in silica phases. The diagenetic boundary between sediments containing biogenic opal-A and those containing opal-CT forms a distinctive lithologic and seismic marker at all sites. Opal-A is the primary silica phase in uppermost Miocene to Quaternary sediments. Opal-A is transformed to diagenetic opal-CT below depths of about 215–325 mbsf, in sediments ranging in age from about 5 to 8 Ma at the Leg 127 sites. The estimated temperature at the opal-A/opal-CT boundary at the four sites ranges from 36° to 43°C. A transition from opal-CT to quartz occurs about 325–471 mbsf in sediments 8–14 Ma old at these sites. The estimated temperature of this transition at these localities is 49°–62°C.

Biostratigraphy

The distribution of microfossils in sediments recovered from Sites 794, 795, 796, and 797 of the Japan Sea is controlled by both post-depositional processes and environment at the time of deposition. The opal-A/opal-CT transformation affects the distribution of diatoms and radiolarians at all the sites. Diatoms and radiolarians are most abundant and best preserved above the boundary where the distribution and condition of siliceous microfossils reflects environment at the time of deposition. In upper Miocene and Pliocene sequences, diatom ooze and diatom silts and clays were produced by high productivity, and in upper Pliocene and Quaternary sections, siliceous microfossils are variable in preservation and abundance in response to glacial cycles in productivity and water-mass conditions. Radiolarians also vary greatly in assemblage composition at this time.

Siliceous microfossils decline rapidly in abundance below the shallowest occurrence of opal-CT. Diatoms disappear within 10–20 m below the boundary, but frustules are occasionally preserved in some carbonate concretions below the transition. Radiolarians, which appear coated with opal-CT, frequently persist below the boundary in low abundance and poor condition.

Carbonate microfossils are, in general, poorly preserved in sediments of the Japan and Yamato Basins. Calcareous nannofossils and foraminifers are best preserved in upper Quaternary sequences where authigenic carbonate formation is minor. Variability in abundance and preservation is likely controlled by changes in water-mass character, including the carbonate compensation depth (CCD), during Quaternary glacial cycles. Calcite fossils are also preserved in middle Miocene sequences where calcium in pore waters is high in concentration due to diffusion from underlying basaltic rocks. Preservation may also be related to warm middle Miocene climatic conditions. The occurrence of calcareous microfossils in lower Quaternary, Pliocene, and upper Miocene units is sporadic. Carbonate microfossils, mostly benthic foraminifers, seem little affected by the opal-A/opal-CT transition, which tends to restrict diagenetic reactions driven from basement. Carbonate microfossils are both preserved in and absent from intervals above and below the boundary, and the importance of post-depositional diagenesis relative to dissolution below the CCD prior to final burial is unclear at this time. Carbonate preservation is better at Site 797 in the southern Yamato Basin than in sections from more northerly sites.

The diatom zonation of Koizumi (1985) and Koizumi and Tanimura (1985) best divides upper Miocene to Quaternary sequences encountered above the opal-A/opal-CT boundary, and is useful below this boundary where diatoms are preserved in carbonate concretions. The zonation, which was defined in the high-latitude North Pacific Ocean, needs no significant revision for application in the marginal sea setting (Fig. 12).

No previously defined radiolarian zonation adequately describes sections recovered at Leg 127 sites in the Japan Sea. Neogene and Quaternary radiolarians are sufficiently abundant, diverse, and preserved for biostratigraphic application above the opal-A/opal-CT boundary. Nevertheless, many known biostratigraphic markers are sporadic in occurrence, absent from the Japan Sea sequences, or diachronous with other sites. Radiolarians, unlike phytoplankton which are restricted to the photic zone, include many species that live at intermediate water depths. Many species are excluded from the marginal sea due to water-mass differences caused, in part, by shallow bathymetric sills. A preliminary zonation was used to describe the Leg 127 sites (Fig. 12).

The tropical and subtropical calcareous nannofossil zonations of Bukry (1978) and Rahman and Roth (1989) adequately describe Quaternary and middle Miocene sequences where nannofossils are preserved. Some zones could not be differentiated, however, because critical warm-water species were excluded from the cool Japan Sea. No fossil floras from the Pliocene and late Miocene could be assigned to zones due to absence of warm-water species which define zonal boundaries.

Planktonic foraminifers younger than middle Miocene in the Japan Sea comprise low-diversity, subpolar assemblages of long-ranging species. Early to middle Miocene faunas contain two short ranging species, but diversity and numbers of specimens are small and preservation is poor. Zonal assignments are not possible in core-catcher samples from Leg 127 Sites.

The microfossil assemblages provide clues to the oceanographic and climate history of the Japan Sea from the early and middle Miocene to the present (Fig. 13). Based on planktonic foraminifers and calcareous nannofossils, the Japan Sea cooled to a temperate to subpolar biogeographic province in the middle Miocene. The northern Yamato Basin (Site 794) and the northern (Site 795) and eastern (Site 796) margins of the Japan Basin deepened from upper middle (500 m) to lower middle bathyal (>1500 m) paleodepths between the middle and late Miocene. In contrast, the southern Yamato Basin (Site 797) had subsided to near 1,500 m by middle Miocene and reached depths greater than 1,500 m by the latest Miocene.

High productivity persisted in the Japan Sea from 8 to 2 Ma as in other marginal basins of the Pacific rim based on the presence of diatom ooze, diatom clays, and diatom silty clays. Sea ice formed in the northern Japan Sea in short episodes at 4.5–4.4 Ma at Site 795 and at 4.0 Ma at Site 796 prior to the onset of northern hemisphere glaciation 2.5 Ma. Sea ice reappeared between 2.7 and 2.4 Ma at Site 795 and at 2.3 Ma at Site 796, and

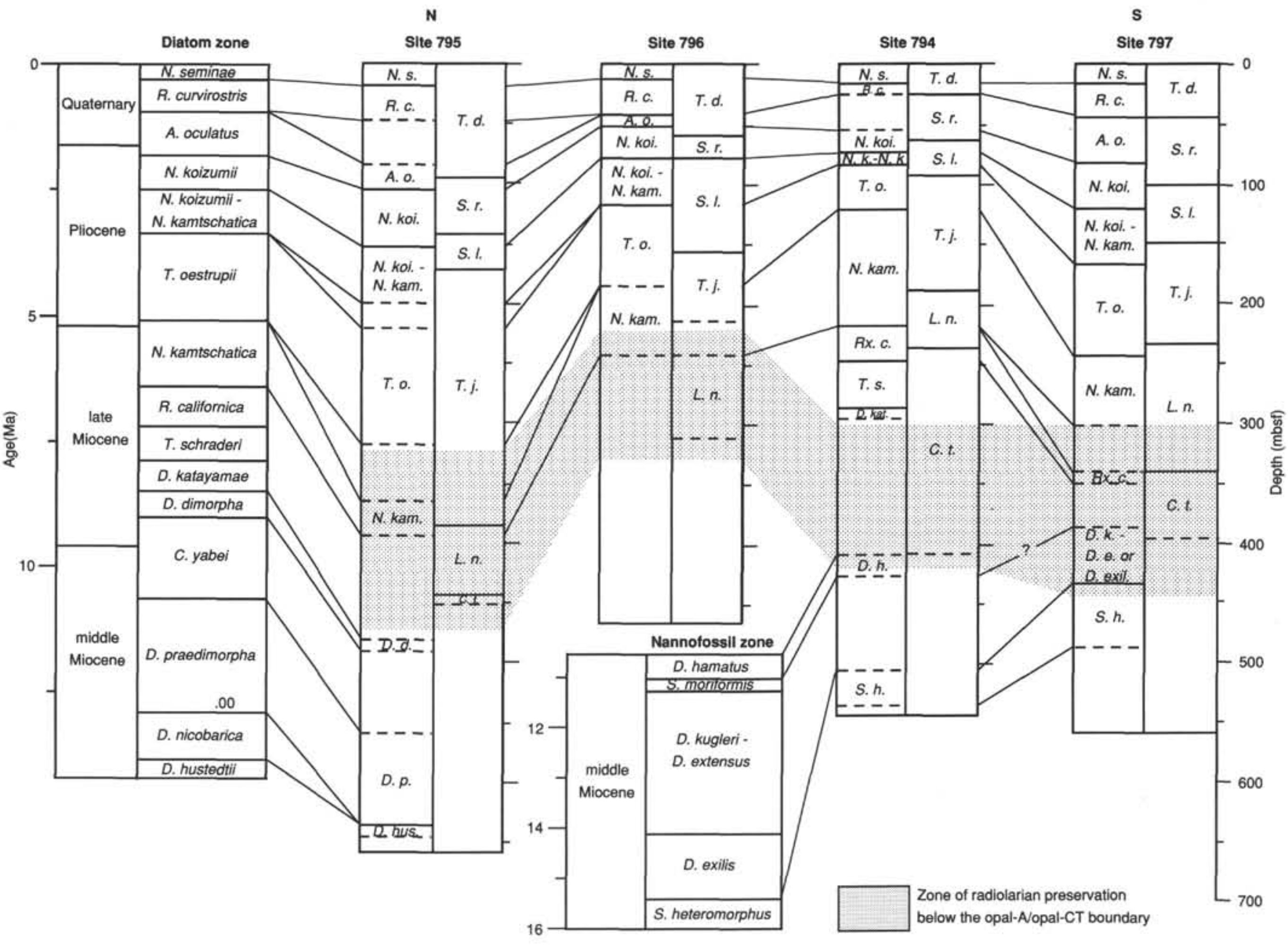

Figure 12. Biostratigraphic summary of zones used at Leg 127 sites. The preliminary radiolarian zones are compared to diatom and calcareous nannofossil zones to assess synchroneity of radiolarian zonal boundaries. T. d. = *Theocalyptra davisiana* zone; S. r. = *Sphaeropyle robusta* zone; S. l. = *Sphaeropyle langii* zone; T. j. = *Thecosphaera japonica* zone; L. n. = *Lychnocanium nipponicum* zone; C. t. = *Cyrtocapsella tetrapera* zone.

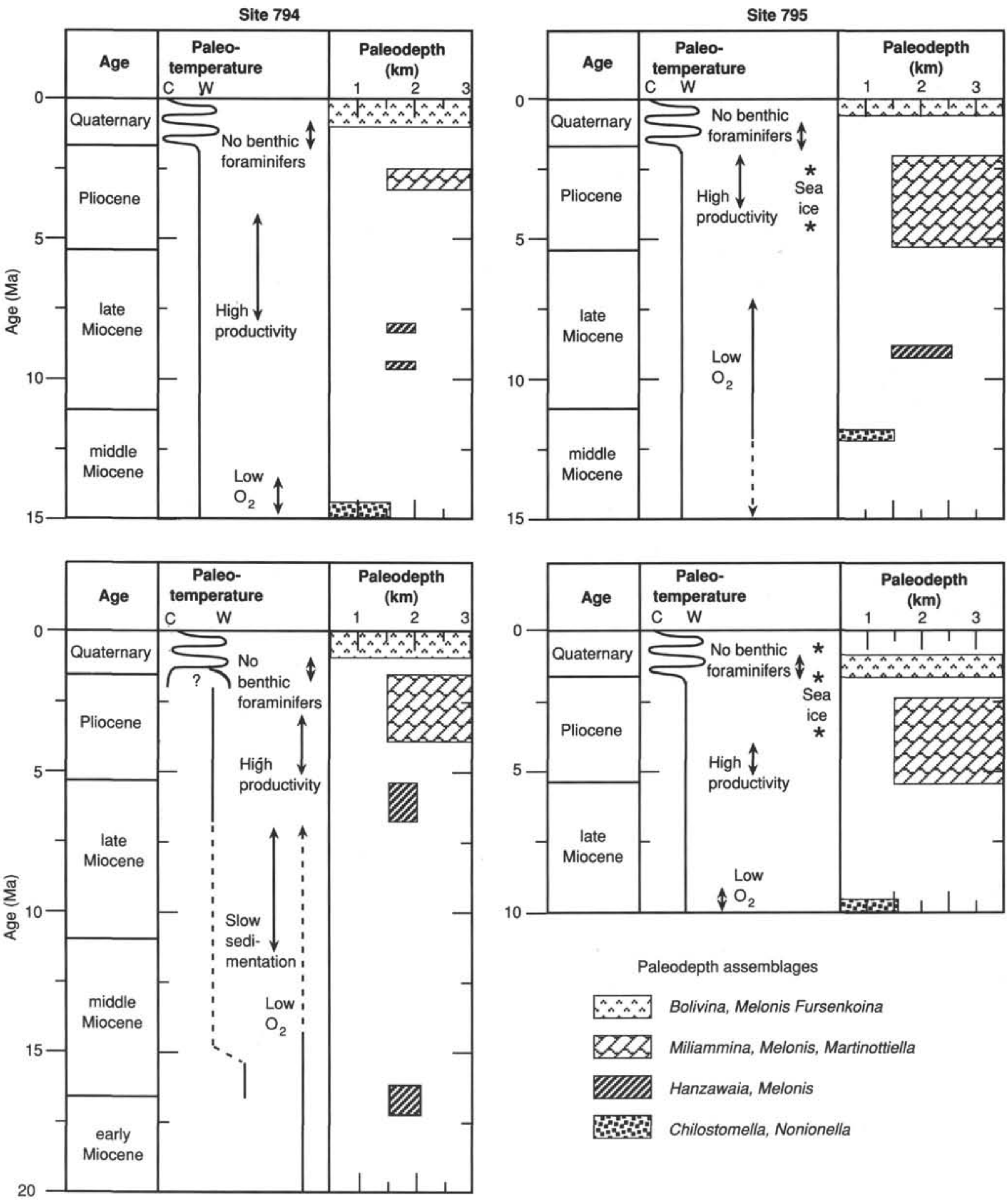

Figure 13. Paleoceanographic summary of Leg 127 sites.

between 0.9 and 0.7 Ma at Site 796 based on occurrences of sea-ice diatoms.

Early Quaternary deep water in the Yamato and Japan Basins was unsuited to benthic foraminifers based on their absence from units in which planktonic foraminifers and calcareous nannofossils are preserved. Late Quaternary water-masses fluctuated in response to glacial cycles based on variability in assemblage composition, preservation, and abundance of radiolarians, planktonic foraminifers, and calcareous nannofossils.

Paleomagnetism

Magnetostratigraphy was the major objective of the paleomagnetic study during Leg 127. The natural remanent magnetization (NRM) of the archive halves of the recovered cores was measured and demagnetized with the pass-through cryogenic magnetometer. The intensity of the magnetization of the sediments is quite low and ranges generally between 0.5 and 5 mA/m in the NRM. After alternating field (AF) demagnetization in a peak field of 15 mT, this value decayed below 0.1 mA/m.

The magnetostratigraphic record of the sediments was better in the Yamato Basin (Sites 794 and 797) than in the Japan Basin (Sites 795 and 796). A correlation of the polarity pattern observed at Sites 794, 795, and 797 with the Geomagnetic Reference Time Scale (GRTS) is shown in Figure 14. At Site 796, gas disrupted the core in the upper part of the hole resulting in scattered directions. This condition, coupled with poor core recovery and lack of paleontological control in the lower part of the hole, made it difficult to obtain a coherent magnetostratigraphic record.

The best magnetostratigraphic record was found at Hole 794A. All chrons and subchrons existing in the GRTS, from the Brunhes to the Gilbert chron (0–5 m.y.) were identified. At Sites 794 and 795, the Brunhes/Matuyama boundary showed a multiple reversal of the magnetic field; a similar behavior of the field has been recently found in Japan by Okada and Niitsuma (in press).

Most of the usable paleomagnetic results obtained during Leg 127 correspond to the intervals cored with the APC. The pass-through cryogenic magnetometer works well with core containing minimal drilling disturbance. In contrast, erratic directions and remagnetizations hampered the ability to define a polarity pattern in the lower part of the holes, and the 15 mT demagnetization allowed in the cryogenic magnetometer was not always sufficient to completely remove the overprints. The XCB drilling in particular produced a deformation of the cores that made measurements of the remanent magnetization of limited usefulness. The low intensity of the remanence did not permit the study of a consistent and reliable number of discrete samples to clarify the characteristic remanent magnetization of the rock.

Except at Site 796, the intensity of NRM, the magnetic susceptibility, and the isothermal remanent magnetization (Site 797 only) showed higher values in the upper parts of the holes. Paleomagnetic results from the two sites in the Yamato Basin (Sites 794 and 795) with different sedimentation rates deteriorate at about the same depth. This observation implies that diagenetic processes influence the magnetic properties of these sediments more than the sedimentary processes. Decrease in the grain size and replacement of primary magnetite with iron sulfides under reducing condition during suboxic diagenesis of organic matter have been recognized in deep sea sediments (Froelich et al., 1979; Karlin and Levi, 1983, 1985; Canfield and Berner 1987). Widespread occurrence of pyrite testifies that reducing conditions and iron sulfides exist in the Japan Sea (Kobayashi and Nomura, 1972). These conditions suggest that diagenetic processes may account for the poor magnetostratigraphic record observed below a certain depth. Other processes, such as increased amounts of volcanic ash varying degrees of bioturbation, may also have played a role.

Sediment Accumulation Rates

Estimates of sedimentation rates for Leg 127 sites are based on diatom datums and paleomagnetic reversal stratigraphy above the opal-A/opal-CT boundary. Below this diagenetic boundary, age control is provided mainly by sparse calcareous nannofossils and planktonic foraminifers. In addition, some diatom datums are preserved in carbonate nodules and layers which are present below the opal-A/opal-CT transition at Site 795. Except for this site, the sedimentation rate curves are better constrained in the upper parts of the sections (Fig. 15).

Sedimentation rates are variable and show few trends. The highest rates occurred in the late Miocene of Site 794 (49 m/m.y.), the Pliocene of Site 795 (77 m/m.y.), the Quaternary of Site 796 (74 m/m.y.), and the late Miocene of Site 797 (56 m/m.y.). Rates below the opal-A/opal-CT boundary are 10 to 25 m/m.y. slower than those above the boundary at three sites, Sites 795, 796, and 797, but there is no difference above and below the boundary at Site 794. Exceptionally slow rates are evident from two cores, in the basal Quaternary section of Site 796 (9 m/m.y.) and in the upper and middle Miocene section of Site 797 (5 m/m.y.). These intervals are shortened by unconformities.

The age of the acoustic basement at each site was estimated by extrapolating the sedimentation rates in the overlying claystones (Fig. 15). Accordingly, the top of the dolerite sills at Site 794 is estimated at 14.8–16.2 Ma. The top of the brecciated basaltic andesite at Site 795 has an estimated age of 13.0–15.0 Ma. Similarly, the age of the shallowest basalt at Site 797 is 16.0–20.0 Ma. Site 796 terminated at 465 mbsf, about 115 m above basement. Extrapolating the average sedimentation rate of 42 m/m.y. to 580 mbsf gives an estimate of 16.7 Ma for the top of acoustic basement at this site.

Inorganic Geochemistry

The interstitial water chemistry program on Leg 127 revealed five different processes responsible for the concentration profiles of the major and minor ions analyzed. Three of these processes operate between the sediment/water interface and the opal-A/opal-CT transition zone, and two at or below this chemical and physical boundary. These controls are summarized below according the depth intervals in which they dominate the interstitial water chemistry.

Bacterial degradation of organic matter is a key process which controls interstitial water chemistry at shallow depths. Sulfate reduction is occurring at all sites due to the availability of metabolizable organic matter. At Sites 795 and 796, in the northeastern Japan Basin, sulfate is totally depleted at 80 and 15 mbsf, respectively, below which methanogenesis begins. Methane-clathrates influence the uppermost pore-water chemistry at Site 796. At Sites 794 and 797, both in the Yamato Basin, sulfate is present throughout the sedimentary column, and methanogenesis is of minor importance. These differences may reflect basinal differences in the rates of supply, preservation, and composition of organic matter. Bacterial sulfate reduction is accompanied by increases in alkalinity and ammonia. Phosphate is released in the upper sediments and removed at depth.

Alteration of volcanic ashes is a second important process occurring at shallow depths. Frequently occurring ash layers in the Quaternary sections of all sites are involved in diagenetic alteration reactions, which include removal of Mg, K, and Rb, and the release of Ca during clay-mineral formation.

A third significant process is the formation and alteration of carbonate minerals. This process influences the pore-water dis-

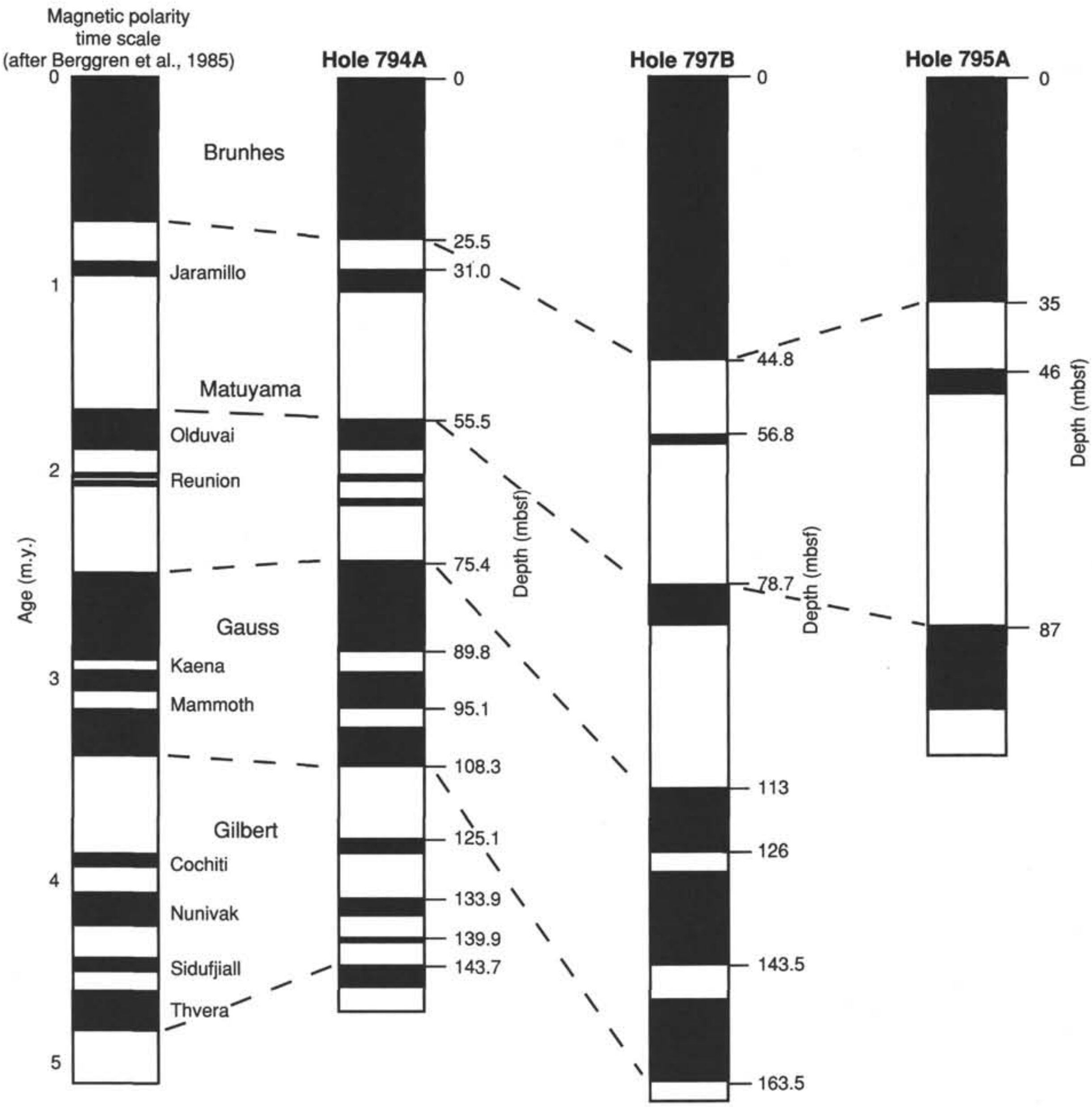

Figure 14. Polarity interpretation of the paleomagnetic results at Sites 794, 795, 797, and correlation with the magnetostratigraphic time scale of Berggren et al. (1985).

tribution of Ca, Mg, and often Sr, at all Leg 127 sites. Dolomite may be forming both directly from solution and at the expense of a calcium carbonate precursor. At depth, diffusion from and into altered basement obscures the chemical signature of carbonate formation.

Silica diagenesis is one of the most conspicuous and dominant process at work in all Leg 127 sites. The opal-A/opal-CT transformation overprints virtually all profiles, and effectively divides each site into two diffusive regimes. The concentration of silica in the interstitial waters reflects the abundance of biogenic silica in the upper sedimentary column and indicates the position of the opal-A/opal-CT transition zone. Porosity and permeability reductions across the silica phase transition profoundly affect pore-water concentration gradients by impeding diffusion through the sediment column. Interstitial waters above the opal-A/opal-CT transition are strongly influenced by communication with seawater; those in pore waters below the transition are influenced primarily by basement alteration reactions.

Basement alteration reactions dominate chemical behavior at depth, and are manifest most notably by the almost complete removal of Mg from pore waters and the concomitant release of Ca and Sr into these waters. Basement rocks are a sink for K, Rb, and Li.

Organic Geochemistry

The Japan Sea sediments contain predominantly low concentrations of calcium carbonate (<1%). Thin intervals of higher carbonate content (up to 74%) occur periodically and are most frequent at Sites 794 and 797 in the Yamato Basin. At Sites 795 and 796 in the Japan Basin, carbonate concentrations significantly above 1% occur mainly in the Quaternary sediments and in the upper Miocene section (Site 796).

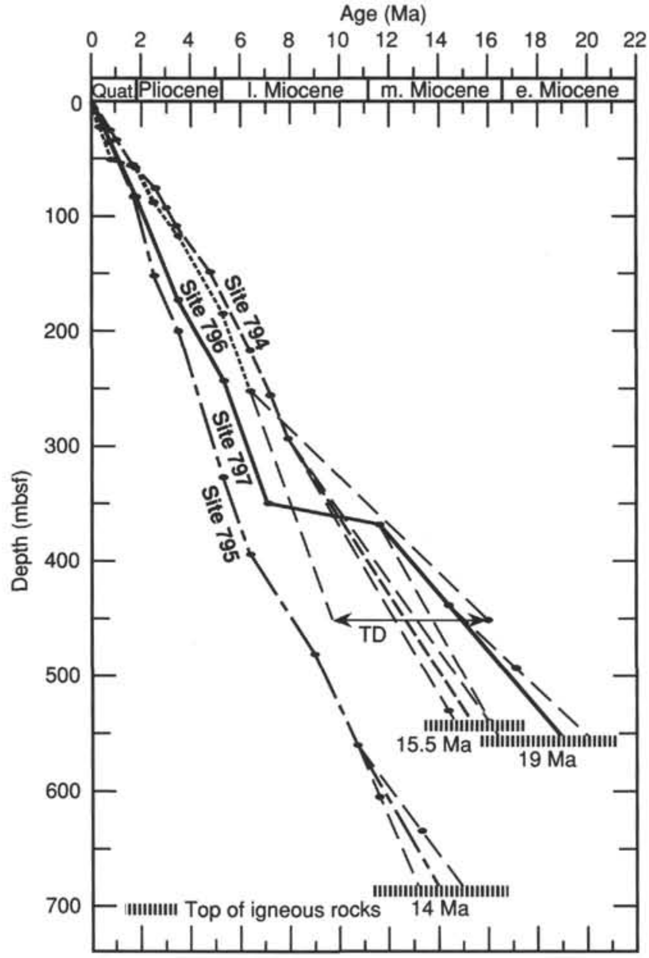

Figure 15. Summary of sedimentation rates (age vs. depth) at Leg 127 sites.

The concentrations of organic carbon (C_{org}) in the sediments of the Japan Sea are most variable in the Quaternary sediments, ranging from 0.02% to 7.4% with an average of 1.3%. In contrast, organic-rich intervals are scarce in the Pliocene sediments, with C_{org} rarely exceeding 1.0%. The Miocene sediments of the Japan Basin (Sites 795 and 796) are similarly low in organic carbon, but coeval upper Miocene sediments in the Yamato Basin (Sites 794 and 797) contain common intervals of very high organic matter, with C_{org} ranging between 0.33% and 8.5%. The rest of the Miocene sediments in the Yamato Basin are low in organic carbon and comparable to those of the Japan Basin.

Methane concentrations in sediments of Sites 794 and 797 in the Yamato Basin are very low. In contrast, sediments at Sites 795 and 796 in the Japan Basin have high concentrations of biogenic methane; in fact, gas hydrates were recovered at the latter site. Thermogenic sources of methane and ethane appear to be minor at all the sites.

The low concentrations of calcium carbonate and relatively poor preservation of biogenic carbonate indicate that the CCD was generally shallow throughout most of the Neogene and Quaternary in the eastern Japan Sea. The most frequent fluctuations occurred during the Quaternary. The slightly higher contents and better preservation of carbonate at Site 797 suggest occasional downslope redeposition of sediments from the nearby Yamato Rise, which currently lies above the CCD. Some of high carbonate values in the sediments, particularly at moderate burial depths, are a result of formation of authigenic dolomite; others may reflect brief episodes of increased productivity and preservation in the Japan Sea.

Relatively large fluctuations in C_{org} are found in the ubiquitous interlayered light- and dark-colored silty clays that are characteristic of the Quaternary sediments found at the four drill sites. The frequent occurrences of these light and dark bands do not necessarily correlate between the adjacent sites. The dark, organic-rich layers may relate to episodic high productivity coupled with enhanced preservation due to low bottom-water oxygen contents. Alternatively, organic matter originally preserved in slope or shelf sediments in areas of depleted oxygen or higher productivity may have been redeposited in the basinal settings of Sites 794, 795, and 797. The latter process is consistent with the preliminary indications of increased terrestrial organic matter in the dark organic-rich bands. The low C_{org} in most of the Pliocene and Miocene sediments suggests that well-oxygenated bottom waters dominated during these periods. The section containing high C_{org} intervals in the upper Miocene sediments of Sites 794 and 797 reflect changes in either productivity or preservation that were unique to the Yamato Basin. Such a difference between the Yamato and Japan Basins during the late Miocene suggests that either limited upwelling occurred or that the deep-water circulation was such that the bottom-water oxygen content of the Yamato Basin was severely depleted relative to that of the Japan Basin.

The high amounts of biogenic methane in sediments of the Japan Basin and, conversely, the low values in Yamato Basin sediments are consistent with the observed rapid depletion of pore water sulfate in the shallow sediments of the Japan Basin and its continued presence at greater depths in the Yamato Basin. Although the overall organic carbon contents at all the sites are similar, the higher sedimentation rates in the Japan Basin may have led to better preservation of the carbon which is easily metabolized by anaerobic bacteria. High oxygen contents in bottom waters and slower sedimentation rates would have allowed more efficient aerobic degradation in the Yamato Basin, thereby leaving less available for the sulfate-reducers and methanogens.

Basement Rocks

Igneous rocks were recovered at three sites. Drilling at Site 794 recovered aphyric to highly plagioclase phyric basaltic and doleritic sills of tholeiitic composition intruded into and chilled against claystone and tuffaceous sediments. At Site 795 drilling recovered massive to brecciated, sparsely plagioclase and clinopyroxene phyric calc-alkaline basalt and basaltic andesite lava flows. At Site 797, drilling penetrated an uppermost suite of predominantly aphyric, brecciated to massive basaltic lava flows interbedded with claystone and a lower suite of predominantly aphyric basaltic and doleritic sills intruded into and chilled against laminated sandstones, siltstones, and claystones. The upper nine units of igneous rocks at this site are high-Al basalt, but the lower analyzed intrusive units comprise mildly alkaline basalt and incompatible element enriched tholeiites.

Some samples from Sites 794 and 797 are quite primitive, with the fresher samples yielding MgO, Ni, and Cr contents as high as 10%, 170 ppm, and 400 ppm, respectively. With the exception of the Site 797 lower suite, all samples are characterized by high Al_2O_3 contents. The high Al_2O_3 of the more evolved basalts could partially be explained by the suppression of plagioclase crystallization relative to mafic phases caused by moderate contents of magmatic water (e.g, >0.5%; Michael and Chase, 1987). The high SiO_2 and low TiO_2 contents of the basaltic andesites from Site 795 may reflect magnetite crystallization.

The variation in the incompatible element contents of the Leg 127 samples (Fig. 16), particularly in Nb, requires that several distinct sets of parental magmas are required to produce the Leg 127 suite. When normalized to N-type MORB (Sun et. al.,

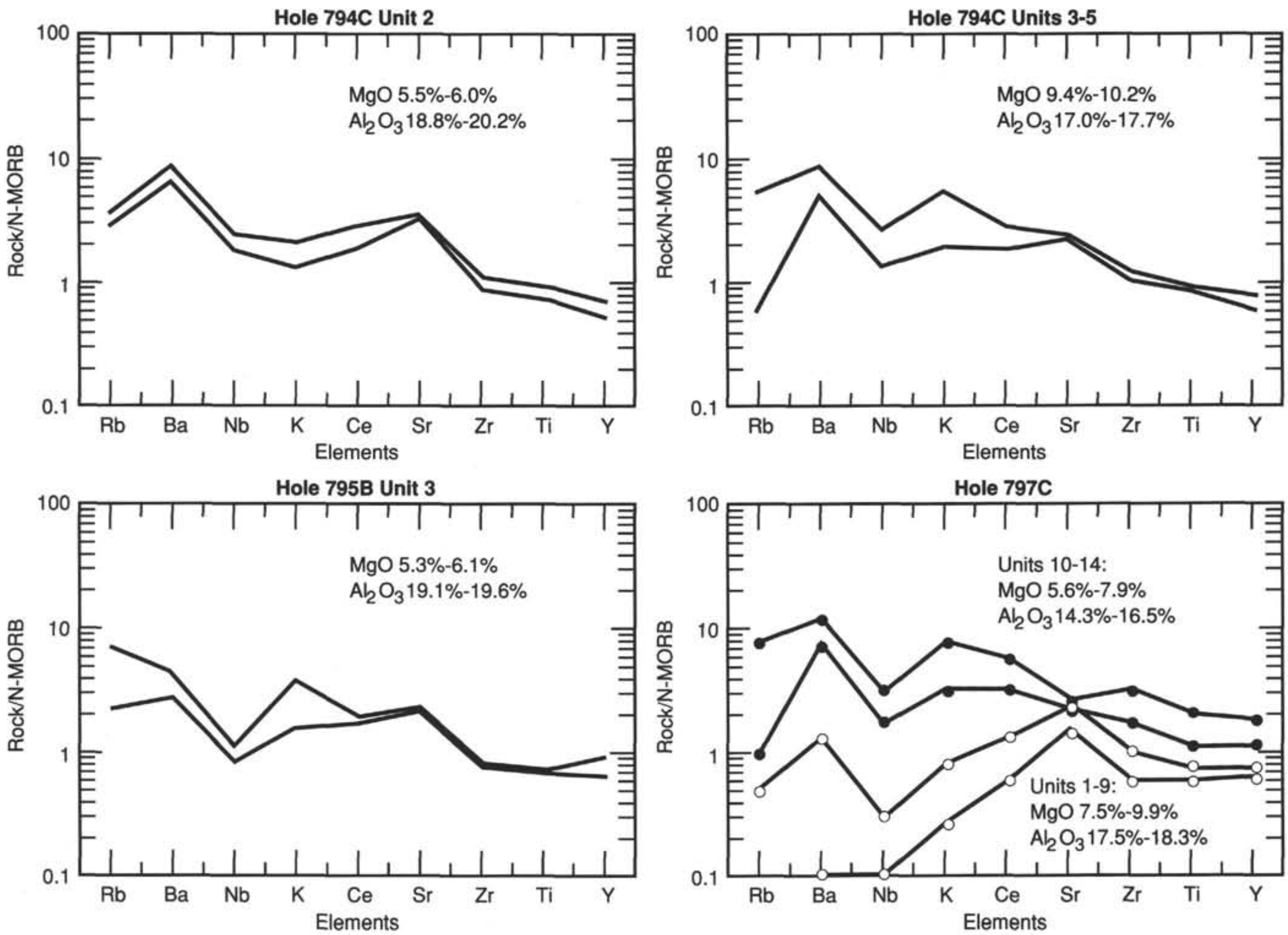

Figure 16. Ranges in N-MORB normalized composition for relatively unaltered samples from various units from all sites penetrating acoustic basement. The absolute range in MgO and Al_2O_3 is also shown. Normalization factors are from Pearce et al. (1981). Rb, Ba, and K analyses may not be representative of original magma composition because of alteration. The data are from shipboard XRF analyses.

1979), rocks from Sites 794 and 795 show a general enrichment in the large ion lithophile elements (LILE; Rb, Ba, K, and Sr) and Ce relative to the high-field-strength elements (HFSE) Zr, Ti, and Y. The high-Al basalts and dolerites from Site 797 lack this pattern of enrichment. With the exception of the lower suite from Site 797, the igneous rocks from all sites show a relative enrichment in Sr, and the rocks from Sites 795 and 797 show a strong relative depletion in Nb. The moderate water contents suggested by the high Al_2O_3, the lack of a significant iron-enrichment trend, the enrichment in Sr relative to mid-ocean ridge basalts (Fig. 16), and the relatively low Nb contents indicate that the basalts and basaltic andesites from Site 795 and from the upper suite of Site 797 share compositional affinities with other arc basalts and andesites (e.g., Gill, 1981). However, the low LILE and Ce contents imply that little continental material was involved in the genesis of these lavas, and that crust of continental character may not underlie these sites. The rocks from Site 794 lack the relative depletion of Nb, and are similar in composition to other back-arc basin basalts (e.g., Saunders and Tarney, 1984). These compositional relations are consistent with the relative locations of Sites 794 and 797 in the Yamato Basin; Site 794 lies in the center of the basin, whereas Site 797 lies on the basinal margin, closer to the edge of the former arc.

The moderately alkaline basalts and enriched tholeiites from the lower suite of Site 797 are quite different from the other igneous rocks. They contain relatively high amounts of the alkalis, LILE, and Ce as well as high amounts of the HFSE. These rocks resemble lavas associated with mid-plate volcanism and rifting, and were derived from a very different source than the nonalkaline rocks. The intrusive nature of the units precludes an absolute determination of the relative time of their genesis.

The probable tectonic scenario of the magmatism at all Leg 127 sites is that of a rifting submarine volcanic arc. The occurrence of interlayered sediments and sills is similar to that found by drilling in other back-arc basins (e.g., Dick et. al., 1980; Stoeser, 1975; Donnelly et. al., 1973) and is a confirmation of the prediction made by Tokuyama et. al. (1987) that large portions of the Yamato Basin are underlain by sediment/sill complexes. This finding has important implications for hypotheses regarding the Yamato Basin formation processes, and suggests that intrusion of sills into sediments during basin formation may help to explain the anomalous crustal thickness of the Yamato Basin, a process similar to that proposed by Einsele (1982) for the Guaymas Basin in the Gulf of California.

Physical Properties

Profiles of water content vs. depth dramatically illustrate the nature and significance of physical properties measurements for rocks and sediments recovered at Leg 127 sites (Fig. 17). In the sediments, profiles of all physical properties reflect the primary

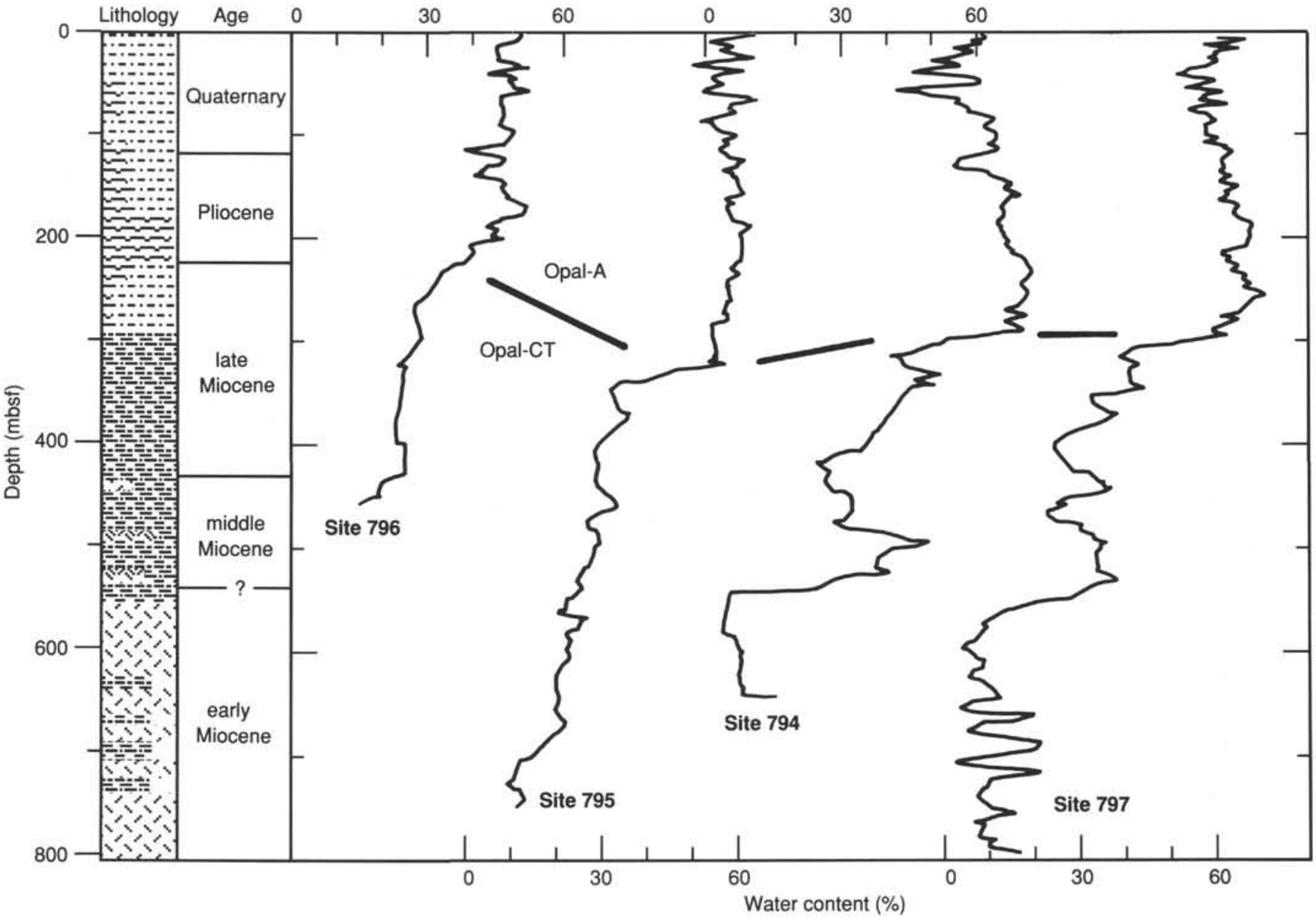

Figure 17. Water content vs. depth for Sites 794, 795, 796, and 797. The summary lithologic section for Site 797 is representative of all sites except Site 796 and is included for reference. Note individual scales for each site. The curves represent the five-point tapered running mean. Outliers that are representative of rare lithologies have been removed.

compositional differences and diagenetic alteration and can be correlated with changes in the pore-water and sediment chemistry. In the volcanic rocks, physical properties correlate with degree of alteration and vesicularity.

The profiles are remarkably uniform in the diatomaceous intervals down to the opal-A/opal-CT boundary at all sites. The data show that the diatomaceous sediments undergo little or no compaction at shallow burial depth, probably a reflection of the strength of the diatom frustules. Across the diagenetic transition from opal-A to opal-CT where the diatoms undergo dissolution and reprecipitation, the physical properties show large and abrupt changes. Below this boundary, the sediments appear to undergo normal compaction, with generally decreasing water content and porosity, and increasing bulk density, acoustic velocity, and thermal conductivity. The marked and distinct response of the physical properties to the opal-A/opal-CT diagenetic transformation may be correlated with the thermal gradient measurements to define a major thermal and seismic marker horizon in the Japan Sea.

In the igneous rocks, higher values of water content, and correspondingly lower bulk densities and acoustic velocities, correlate with the most altered or most vesicular rocks. At Site 797, sediments are interbedded with the igneous units. These interbedded sediments have higher water contents than the surrounding basalts, but have significantly lower water content than the sediments overlying basement. These interbedded sediments are either abnormally consolidated and compacted or have been thermally altered through contact and interaction with the basalts.

The data from Sites 794 and 797 have been juxtaposed to illustrate the striking similarity of the two profiles. The two sites are from opposite ends of the Yamato Basin; Site 797 is near the Yamato Rise, and has a higher degree of terrigenous input. Nevertheless, the similarity of the two profiles indicates that the physical properties are controlled by processes that are acting basin-wide.

The character of the data profile from Site 796, located on the Okushiri Ridge, is different from the other sites. Recent tectonic activity has apparently affected the physical properties of the sediments at this site. The opal-A/opal-CT transition, which is sharp and notable at the other sites, is diffuse and occurs at shallower depths (about 215 mbsf vs. about 300 mbsf) at Site 796. These characteristics may reflect rapid readjustment of this diagenetic front related to uplift and higher heat flow beginning about 1.8 Ma.

Thermal Gradients and Heat Flow

An intensive temperature measurements program was executed at all of four Leg 127 sites and successful measurements of thermal gradient were accomplished (Fig. 18). Temperature measurements, together with careful and accurate measurements of thermal conductivity, provided fully reliable heat flow data at the four sites. Accurate heat flow measurements in the upper

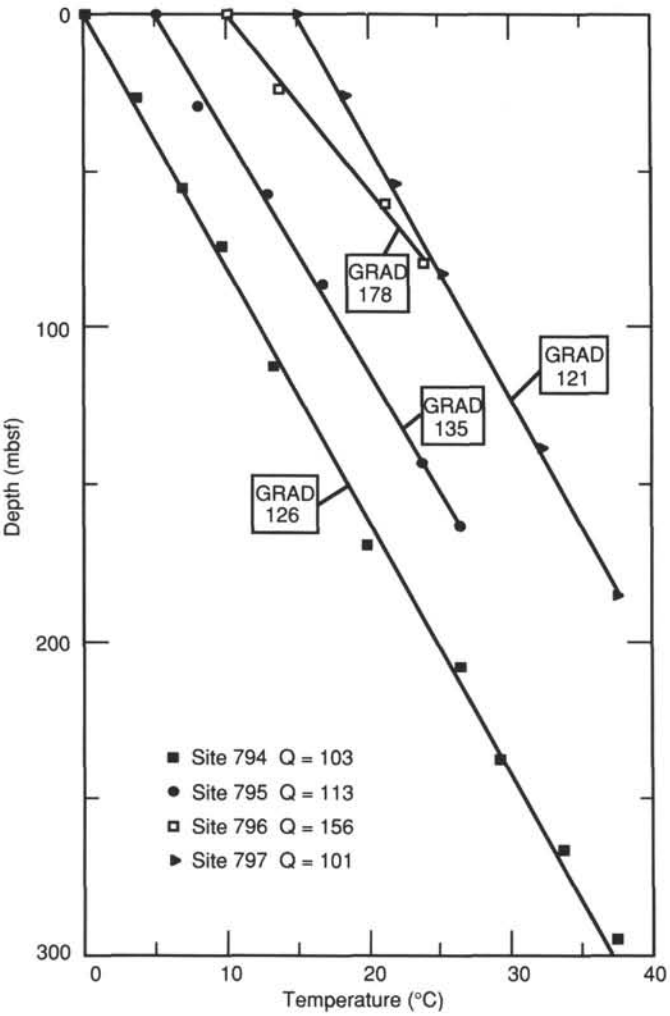

Figure 18. Summary of downhole temperatures measured at the four Leg 127 Sites. Note the temperature profiles for Sites 795, 796, and 797 have been displaced by 5°C, 10°C, and 15°C, respectively, from their true temperature to prevent overlap in the figure.

200–300 m of sediment combined with measurements of the thermal conductivity provided good estimates of the temperature profile to the total depth of each hole. These profiles greatly aided the study of silica diagenesis and were useful guides in the safety considerations concerning thermal maturity of deeper part of sedimentary column at the drilling sites.

Measurements at Site 794 and Site 797 in the Yamato Basin yielded heat flows of 103 and 101 mW/m^2, respectively. These values are in excellent agreement with nearby seafloor measurements and only slightly higher than the average of seafloor measurements in the Yamato Basin (Tamaki, 1986). Site 795 is in the northeastern corner of the Japan Basin. The heat flow measured there, 113 mW/m^2, is higher than the mean of nearby seafloor measurements, and significantly higher than the average heat flow in the Yamato Basin. The temperature profiles at these three sites are linear within measurement error, indicating that the mode of heat transfer is conductive and that there are no significant sources or sinks of heat in the intervals measured.

Site 796 on Okushiri Ridge provided an opportunity to measure heat flow over an apparently young plate boundary, thought to have developed within the past 2 m.y. Existing heat flow data over this zone is sparse, and no prior measurements had been made over Okushiri Ridge. The heat flow measurement at Site 796 on the eastern flank of Okushiri Ridge yielded a value of 156 mW/m^2, which is one of the highest values ever measured in the Japan Sea. It indicates an excess heat flow of about 40 mW/m^2 over this currently active tectonic feature. The ultimate source of much of this excess heat flow must come from energy dissipated by the ongoing deformation. Most of the downhole temperature measurements at Site 796 were disturbed by penetration of permeable sediments at the bottom of the hole by cold water circulated during drilling. The three valid temperature measurements at Site 796 do not allow a confident assessment of the mode of heat transfer or heat production in the measurement interval.

The data at all four sites provide accurate estimates of the current *in-situ* temperatures to the total drilled depths. Temperatures at the opal-A/opal-CT transition fall in the range 36°–43°C; the opal-CT/quartz transition is in the range 49°–62°C. The opal-A/opal-CT boundary is a distinctive reflector in seismic reflection sections in the Japan Sea, and, where present, can be used as a reasonably accurate guide to the variation of temperature gradients and heat flow.

Downhole Logs

A full suite of Schlumberger logging tools and Lamont-Doherty specialty tools were deployed on Leg 127. The Schlumberger tools included the geophysical/lithodensity tool string, the geochemistry tool string, and the formation microscanner (FMS). The Lamont tools included the borehole televiewer (BHTV) and temperature tool. A planned vertical seismic profile (VSP) at Site 794 and two packer experiments planned for Sites 794 and 796 were abandoned because of bad hole conditions.

Nearly the complete sequences of sediments (600 m thick) were logged at the Yamato Basin sites (Sites 794 and 797) using the geophysical/lithodensity, geochemical, and FMS tool strings. Borehole constrictions prevented logging of the full sedimentary sequence at Site 795; only the interval from 100 to 220 mbsf was logged with the geophysical/lithodensity tool string at this site. At Site 796, drilling was terminated before basement was reached. We were able to log two-thirds of the available interval, including the opal-A/opal-CT transition, with the geophysical/lithodensity, geochemical, and FMS tool strings. In addition to the open-hole logging, each run of the geochemical tool string was logged through the casing from the seafloor to 100 mbsf. An exception was Site 797, where the geochemical tool string was run through drill pipe for the full length of the sedimentary sequence. At Site 796, the borehole televiewer was run in a high velocity sedimentary unit. The temperature tool was run attached to the bottom of most of the Schlumberger tool string runs.

At Site 797 difficult hole conditions were encountered. Nevertheless, we were able to obtain data over 30 m of the aphyric basalt/sediment sequence, including data over the sediment/basalt contact, from the FMS and borehole televiewer with the aid of special equipment (the so-called "side-entry sub"), which allowed hole conditioning while logging.

The two sites in the Yamato Basin, Sites 794 and 797, show very similar and rather uniform log responses through the first two sedimentary units and the opal-A/opal-CT transition zone (Fig. 19). Major lithologies in these units are clay, silty-clay, and diatomaceous ooze. Minor ash layers show little or no log response through these first two units. Little change is seen in the sonic velocity log but the resistivity log shows a temperature-related negative gradient. Porosity is nearly constant and high, over 60% through these first two units. Logs from the two holes differ below 350 mbsf in Unit III, coinciding with the onset of XCB coring and poor recovery. At this depth the first layers of chert and porcellanite (5–50 cm thick) occur interbedded with siliceous claystone. The chert and porcellanite have much lower porosities, between 20% and 30%, higher velocities, and resis-

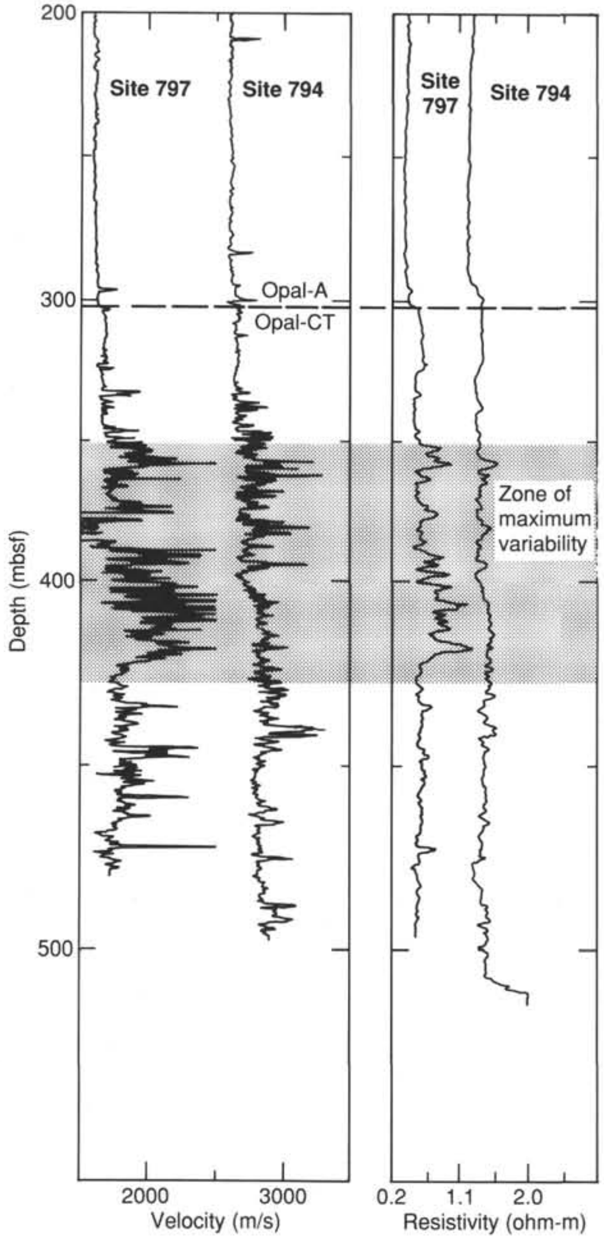

Figure 19. Representative velocity and resistivity logs for selected depth intervals at Sites 794 and 797 in the Yamato Basin.

tivities than the siliceous claystone. The alternating lithologies define a zone of maximum log variability where sharp resistivity and velocity contrasts occur (Fig. 19). The FMS log, which has only been recently modified for slim-hole ODP use, delineates these intervals very well. Our preliminary study of the thickness, frequency, and relative resistivities of the cherty layers at Sites 797 and 794 show that the cherty layers are twice as frequent and much more resistive at Site 797 than Site 794. Below 450 mbsf the sediments at the two sites have similar log responses and lithologies. The limited logs from Site 795 and Site 796 (not shown) are more variable in the coeval upper units, reflecting lower porosity, between 40% and 50%, encountered at these sites. The logs at Site 795 clearly show the presence of dolomite layers.

Site 797 provided our only opportunity to log the basement sequence. These logging operations were hampered by difficult hole conditions caused by swelling clays. After a strong effort, we were able to log only about 30 m of the basement sequence. The two-arm caliper of the FMS tool string demonstrated that the hole diameter varied between 15 and 45 cm over less than half a meter depth. However, sporadic good contact was seen with the FMS, and the gamma ray tool run with the FMS provides information that helps delineate the clay-rich sediments from the aphyric basalt. The BHTV images show vertical, inclined and horizontal fractures throughout the aphyric basalt but no obvious breakouts useful for the determination of stress directions.

Seismic Stratigraphy

The study of seismic stratigraphy at the Leg 127 drilling sites provided fundamental information on the sediments and acoustic basement of the basins of the Japan Sea in terms of age, acoustic character, and interval velocity. Together the four sites constitute key stations needed to tie with the enormous geophysical data base in the Japan Sea.

The correlation of seismic intervals and lithologic units was successfully done at all four sites. Sonic velocity log data provided the most valuable constraint for the correlation. Physical property velocity data, *P*-wave velocities, and Hamilton Frame velocities provided additional or complementary constraints, especially in the intervals lacking log data.

At each site, we identified four or five seismic intervals above the opaque acoustic basement. Direct seismic ties were not made between sites. Nevertheless, the seismic intervals at most sites in basinal areas are broadly similar in seismic character. Diatom ooze represents a transparent interval, and alternating cherts and siliceous claystones below the opal-A/opal-CT diagenetic front represent well-stratified layers, both of which are commonly observed in the basin margin areas of the Japan Sea. Turbidity deposits and relevant seismic intervals were observed at Sites 795 and 796. Deeper penetration into acoustic basement at Site 797 (450 m) clearly revealed the nature of acoustic basement.

The opal-A/opal CT diagenetic boundary is manifested as a set of strong reflectors in the seismic profiles at Sites 794, 795, and 797. This time- and temperature-controlled boundary, which is unequivocally identified in both the lithologic units and seismic intervals, provided crucial constraints for the seismic character analysis at each site. At Site 796, the reflector corresponding to the opal-A/opal-CT transition was not prominent, probably because of ongoing upward and rapid migration of the opal-A/opal-CT diagenetic front caused by heat generation along the compressional tectonic zone of Okushiri Ridge during the Quaternary.

The opal-A/opal-CT diagenetic boundary is parallel to the seafloor and not always coincident with stratal boundaries. At Sites 795 and 796 reflectors corresponding to this boundary cut across those arising from stratal surfaces, demonstrating that the opal-A/opal-CT diagenetic front is not a time horizon in the strict seismic stratigraphic sense (Vail et al., 1977). Instead, the reflectors strongly overprint the original depositional structure and make the interpretation of the depositional history difficult. Despite this aspect, these opal-A/opal-CT reflectors, probably the world's most well-defined and well-documented, provide indispensable information on the thermal history of the Japan Sea.

At Sites 794 and 797, the seismic interval previously identified as acoustic basement was found to be interbedded sediments and basalt sills and flows. These drilling results have helped to reconcile conflicting observations on the seismic velocities of acoustic basement of the Yamato Basin from the wide-angle reflection and multichannel stacking velocities (3500 m/s) and from ocean bottom seismometer refraction studies (4500–

5000 m/s). Our results show a distinct velocity anisotropy of basalts with the vertical propagation direction of seismic waves typically slower than the horizontal propagation direction. The drilling results at Sites 794 and 797 and the vast amount of seismic reflection profiling data of the Japan Sea suggest that this kind of acoustic basement is representative of acoustic basement of most of the deep basins of the Japan Sea. These findings are crucial to unravelling the basement structure of the Japan Sea.

CONCLUSIONS

We achieved three of the four principal objectives of our drilling. They are: determining the age and nature of the basement, determining the sedimentary and oceanographic evolution of the basins, and dating the development of the recent convergent tectonics along the eastern margin of the Japan Sea. We were unable to accomplish our fourth objective, the acquisition of *in-situ* stress measurements, because of unstable hole conditions at all the sites. At three of the four drilling sites (Sites 794 and 797 in the Yamato Basin and Site 795 in the Japan Basin) we penetrated the acoustic basement and recovered the complete overlying sedimentary section. At Site 796 on Okushiri Ridge, the drilling recovered the upper 80% of the sedimentary column. These data provide unequivocal, crucial information on the geology of this marginal basin which developed along an active continental margin. The information gathered includes data from a wide variety of geoscience disciplines which can be tied to an equally large data base in the region. In the discussion that follows, we summarize the conclusions of our Leg, focusing on the tectonic, sedimentological, and paleoenvironmental aspects.

Principal Tectonic Aspects of the Results

Age and Nature of the Basement

We penetrated acoustic basement at Sites 794, 795, and 797. In the Yamato Basin at Sites 794 and 797, we found that the acoustic basement was composed of interlayered basalts and sediments. At Site 797, we drilled 350 m into this interlayered rock and recovered 21 separate basaltic sills and flows. At Site 794, we encountered 1.5 m of tuff and tuffaceous claystone and basalt beneath 100 m of dolerite sills. In the Japan Basin, we reached the acoustic basement at Site 795, but not at Site 796 on Okushiri Ridge. At Site 795, we penetrated 76 m into acoustic basement and recovered brecciated basaltic and andesitic lavas. We may have reached the basement at this site as it is located on a small basement ridge that probably represents a volcanic pile. However, shallow penetration into the acoustic basement at the site does not exclude the possibility that the flows are underlain by sedimentary layers.

Given these findings, we cannot say with confidence that we reached the bottom of the basin sediments at any of the sites of Leg 127. In terms of the age constraints of basin formation, however, these drilling results provide critical information. At all drilling sites, micropaleontological data, specifically rare occurrences of calcareous nannofossils and planktonic foraminifers in the sediments as well as diatoms in dolomite nodules, provided crucial age constraints in the lower part of the sedimentary column. We were able to assign the age of the shallowest sediment/basalt contacts at Sites 794, 795, and 797 according to these paleontological constraints. These are: Site 794, 14.8–16.2 Ma, with the best estimate being 15.5 Ma; Site 795, 13–15 Ma, with the best estimate being 14 Ma; and Site 797, 16–20 Ma, with the best estimate being 19 Ma. Simple extrapolation of the sediment accumulation curve at Site 796, where the drilling was terminated at 110 m above acoustic basement, provides an estimated basement age of 16.7 Ma.

Among these four sites, the results at Site 797 provide the most crucial information about the initiation of the basin formation of the Japan Sea. The sediments just above the shallowest basalt at this site are phosphatic siliceous claystones; the benthic foraminiferal assemblage in this claystone indicates a lower middle bathyal level, suggesting that the basin was already well developed by 19 Ma at this site. As Site 797 is located at the margin of the Yamato Basin, this age provides the first clear evidence that constrains the initial stage of the opening of the Yamato Basin. The younger basal sediment age at Site 794, located at the central part of the Yamato Basin, as well as the forthcoming $^{40}Ar/^{39}Ar$ absolute age data on the basalts, may constrain the age of the final stage of the Yamato Basin opening.

The age of the bottom of the sedimentary column at Site 795 in the northern margin of the Japan Basin indicates that the volcanic activity occurred at 14 Ma in upper middle bathyal water depths, and suggests that the volcanic activity in the Japan Basin lasted at least until 14 Ma. We are uncertain as to whether this volcanic activity is correlated to any stage of the basin formation. Further detailed seismic stratigraphic study and further geochronological and petrochemical studies of the recovered basaltic rocks will help relate the nature of this basement to other basement in the Japan Basin.

One of the principal findings of the Leg is that the acoustic basement of the Yamato Basin consists of interlayered basalts and sediments. This composition was previously proposed on the basis of smooth surface morphology and velocity structure (Ludwig et al., 1975; Tokuyama et al, 1988). Seismic reflection profiling data and sonobuoy wide angle reflection data suggests that similar acoustic basement is probably representative of most acoustic basement of the basinal areas of the Japan sea. As the 3.5 km/s layer (Ludwig et al., 1975) of the wide-angle reflection data may be correlated to this interbedded interval, this interval may be as thick as 0.5–2 km in the basinal areas. Study of this interbedded unit, which is much thicker than the seismically visible upper sediments, unequivocally improves our understanding of basinal structure in this marginal basin.

In conclusion, the drilling of acoustic basement in the Yamato Basin provides good constraints on the age of formation of the Yamato Basin and may partly constrain the age of formation of the Japan Basin. The discovery of the nature of the acoustic basement in the Yamato Basin as revealed by Leg 127 drilling is a crucial achievement toward understanding the structure of the Japan Sea basins.

Style and Dynamics of Opening

The most important finding of our drilling, concerning the style and dynamics of the opening of the Japan Sea, comes from the lowermost sedimentary sequence interlayered with basalt sills and flows at Site 797. The 350 m of drilling below the shallowest basalt recovered lower Miocene sediments indicative of a basin margin slope, gravity-flow-dominated environment. Currently these rocks occur at depths greater than 3500 m below sea level. The lower part of this lower Miocene sequence (lithologic Unit VI) consists of a rhythmically interbedded sequence of fine- to coarse-grained sandstone and siltstone containing abundant plant debris. The character of these sediments reflects rapid sediment accumulation. This sequence suggests that the site occupied a marine slope proximal to a deltaic depositional environment. In contrast, the upper part of this lower Miocene sequence (lithologic Unit V) consists of laminated claystones intercalated with phosphatic carbonate stringers, suggesting an environment isolated from coarse-grained terrigenous sediment input due to a deepened and widened basinal environment. This setting is well supported by the occurrence of benthic foraminiferal assemblages indicative of lower middle bathyal depths.

These strikingly different sedimentary facies are consistent with the rapid subsidence of this part of the Yamato Basin in the early Miocene (probably before 19 Ma). The reconstruction of this sedimentary basin suggests a probable generation of a graben or an initial rift invaded by marine waters some time in the early Miocene and subsequent rapid basin deepening by 19 Ma. The rapid subsidence event that took place at the present basin margin is apparently coeval with the initiation of the opening of the Yamato Basin.

This rifting and the subsequent subsidence event are associated with abundant volcanic activity, as represented by the basaltic rocks that were recovered at Sites 794 and 797. Determination of the radiometric ages and isotopic compositions of the basalts, together with further petrological and geochemical work, will provide critical information on the dynamic interrelationships between basin formation and magmatism.

The igneous rocks at Site 797 consist of high-Al basalt in the upper part of the interlayered sequence, and mildly alkaline and enriched tholeiitic alkaline basalts in the lower part. The sequence of intrusion and extrusion cannot be determined, despite the distinct spatial associations observed. The lower suite of basalts may represent volcanism associated with the early rifting of a continental arc, based on analogy with present-day association of similar basalts with an intraplate setting. Volcanic activity represented by the incompatible-element-poor, high-Al basalts is consistent with the rifting of a continental volcanic arc, where the crust has been ruptured and extended sufficiently so that the lavas have interacted little, if at all, with continental crust. The tholeiitic dolerites of Site 794 contain less of an arc signature and more of a mid-ocean basalt (MORB) signature in their composition than do the high-Al basalts at Site 797. This compositional difference suggests that eruption in the center of the Yamato Basin had occurred after substantial back-arc or within-arc spreading. As seismic stratigraphy suggests widespread occurrence of these sills in the entire Yamato Basin, the intrusion of sills into sediments has played a significant role in the formation of the anomalously thick "oceanic crust" of the Yamato Basin. The subaqueous "blue tuff" beds that were observed at all sites in the middle Miocene sequence may possibly be related to this intense intrusive activity and suggest the occurrence of some submarine volcanoes during the middle Miocene.

Calc-alkaline basalt, basaltic andesite, and basaltic breccia constitute the acoustic basement at Site 795. These lavas share some magmatic compositional affinities with the high-Al basalt at Site 797. This similarity may suggest that the volcanism at Site 795 is also related to the initial stages of arc rifting during initial basin formation. As the estimated age of the Site 795 basalt is 14 Ma, the northernmost part of the Japan Basin may have been initially forming by this time. However, our rather shallow penetration into the basement makes further inferences difficult.

In conclusion, the drilling data suggest that the Yamato Basin formed in the following straightforward manner: (1) initiation of rifting of a continental arc in the middle early Miocene associated with deltaic and basin margin slope marine clastic deposits and alkaline, enriched tholeiitic, and high-Al basalt volcanic activity; (2) basin deepening and the start of widening of the basin in the late early Miocene associated with rapid subsidence and continued intrusion and extrusion of basalt; and, (3) continued, constant basin widening and deepening in the late early Miocene and early middle Miocene with frequent tholeiitic dolerite sill intrusions and probable associated submarine volcanism. The actual mechanism of basin deepening and widening is still unresolved although several possible models may apply. These models include: (1) Guaymas Basin-style dike/sill intrusions associated with seafloor spreading where the sedimentation rate is high relative to the volcanism, or (2) ductile continental (arc) crustal extension focused in the lower crust. The mode of formation of the Japan Basin could not be fully addressed by the onboard synthesis and will depend on further synthetic study.

Quaternary Convergent Tectonics along the Eastern Margin of the Japan Sea

The age of the initiation of the uplift of Okushiri Ridge was determined by the shallowest occurrence of a sand bed. The age of the shallowest sand bed is 1.8 Ma, based on its occurrence near the boundary between the *A. oculatus* and *N. koizumii* Diatom Zones. Below this, abundant occurrences of fine- to coarse-grained sand beds (1–10 cm thick) with sharp basal contacts and grading that suggests a turbiditic origin, were observed in the upper Pliocene unit as well as in the underlying lower Pliocene to upper Miocene units. These depositional data suggest that turbidites were able to reach Site 796 during this time interval, and that Okushiri Ridge did not yet exist. The shallowest appearance of these sand beds at 1.8 Ma indicates that Okushiri Ridge (water depth 2300 m) was uplifted 1300 m above the Japan Basin floor (water depth 3600 m) in 1.8 m.y. at a rate of 0.7 mm/yr. The seismic stratigraphy at Hole 796A suggests that the unconformity exists at the uppermost Pliocene and that this unconformity broadly extends around the site. An unusually slow sedimentation rate of 11 m/m.y. is evidence that further supports the presence of this unconformity apparently related to the uplift of Okushiri Ridge. As the uplift of Okushiri Ridge is caused by thrust activity along the eastern margin of the Japan Sea (a possible new Eurasia-North America plate boundary), these results provide the first exact age data to address the tectonics of this possible new plate boundary.

The highest heat flow ever obtained in the Japan Sea, 156 mW/m^2, was measured at Hole 796B. The associated high temperature gradient (178°C/km) is quite consistent with the shallow, obscured opal-A/opal-CT transition zone (215 mbsf, 38°C). Seismic stratigraphy shows that the depth of opal-A/opal-CT reflector is generally shallower than that of the adjacent Japan Basin, suggesting that anomalous high heat flow is widespread over the Okushiri Ridge. Frictional heating along the thrust faults is one potential source of excess heat, but frictional heat alone cannot account for this high heat flow. A mechanism to concentrate the heat flow, such as fluid flow along faults, is required to match the magnitude of the anomaly. The possibility of vertical flux, however, was not confirmed by the geochemical data of interstitial water data, physical property data, or log data, although all these data show many anomalous vertical profiles of elements and physical properties.

Oceanographic and Sedimentation History

In addition to the tectonic findings, Leg 127 also provided valuable new information and insights to the oceanographic and sedimentological development of the eastern Japan Sea from the early Miocene to the present. In the final sections, we briefly consider these findings in terms of two main aspects, paleoenvironments and post-depositional processes.

Paleoenvironments

The vertical and lateral sequence of sedimentary facies and paleontological assemblages encountered at the four drill sites form the basis for our environmental reconstructions of the Japan Sea. Sites 794, 795, and 797 provide the hemipelagic records most suitable for this purpose. Site 796 allows a glimpse of the interplay of tectonics and sedimentation along the eastern margin of the Japan Sea.

The five regional lithofacies and associated microfossil assemblages reflect the evolution of the deep-sea basins of the eastern Japan Sea from the initial rifting stage, through protracted subsidence, and finally episodic terrigenous input and restricted circulation. Our earliest record of sedimentation is from the southern Yamato Basin at Site 797. The drilling results revealed that in early Miocene time this part of the Japan Sea was probably a narrow shelf and associated slope dominated by clastic sedimentation outboard or seaward of a delta. The sequence consists principally of graded gravity flow and current-reworked volcaniclastic sandstones and siltstones containing abundant, terrestrially derived carbonaceous debris. These strata are intercalated with mafic flows, minor breccias, and shallow intrusive rocks and were probably deposited below wave base and coincident with submarine volcanism during a rifting phase in this part of the Japan Sea.

The second period, beginning in the early Miocene in the Yamato Basin and middle Miocene in the Japan Basin, was characterized initially by moderate to rapid subsidence and deposition of hemipelagic calcareous and siliceous claystone containing carbonate and phosphatic nodules and lenses, minor glauconite, and low amounts of organic carbon mostly below the CCD. Where present, benthic foraminifers and the faintly laminated and moderately bioturbated character of these sediments indicate deposition in suboxic waters at depths of approximately 500–1500 m. Slightly greater water depths (2000 m), warmer surface waters, and variable sedimentation rates occurred in the southern Yamato Basin (Site 797) relative to the northern Yamato Basin and Japan Basin (Sites 794 and 795) during this period, although initiation of this phase of deposition may have been earlier. Seafloor volcanism persisted as evidenced by the ubiquitous occurrence of gravity-flow tuffs.

The third stage spans most of the late Miocene and Pliocene and corresponds to a period of continued subsidence, lowered surface water temperatures, and moderate to poor oxygenation of deeper waters. The sediments that characterize this period are hemipelagic siliceous claystones and diatomaceous silty clay having variable organic carbon contents at the basinal sites (Sites 794, 795, and 797), and mixed hemipelagic claystones and massive, gravity-flow pebbly claystones at the marginal site (Site 796). A significant pulse of organic carbon input and preservation occurred in the Yamato Basin (Sites 794 and 797) during the middle part of the late Miocene. This pulse is not seen in the Japan Basin sites suggesting that barriers to circulation may have existed between the two areas at this time. Water depths in both basinal areas ranged from about 1500 to 2500 m. In addition, the Pliocene sediments are unusually rich in diatoms, suggesting increased productivity during this time.

Cool surface waters persisted during this period and sea ice was present in the northern sites (Sites 795 and 796). Along the eastern margin, pulses of volcaniclastic turbidity currents interrupted the hemipelagic sedimentation. Subsidence also continued during this time, and water depths ranged from 1500 to 3500 m in the northern areas (Sites 795 and 796) and from 1500 to 3000 m in the Yamato Basin (Sites 794 and 797).

The final stage occurred during the latest Pliocene and Quaternary period and brought this sedimentary history to a spectacular finale. At all sites this phase is characterized by a distinctive sequence of interlayered light-and dark-colored silty clays punctuated by volcanic ash. Away from these sites, particularly in the deeper parts of the Japan and Yamato Basins and in the small coastal basins along northern Honshu, this hemipelagic sequence correlates with much thicker sections of terrigenous clastic material derived from uplifted terranes in Japan. In general, the dark-colored layers of the uppermost Pliocene-Quaternary sequence contain more organic carbon and siliceous and calcareous microfossils than the light bands. Both types of layers are variously massive to laminated, and subtle size-grading is common. These characteristics, along with the coeval deposition of coarser clastic material away from the sites, argue for the occurrence of basin-wide oscillations in anoxia and sediment input that must ultimately have been controlled by climate and tectonism. This inference is further supported by distinctive vertical and geographical variations in temperate and subarctic microfossil assemblages which track the temporal climatic changes and demonstrate that the northern locations have remained persistently cooler than the southern sites throughout this period. In addition, variable preservation of planktonic foraminifers in the uppermost Pliocene-Quaternary sediments at most sites suggest a fluctuating CCD. In particular, the early Quaternary period is marked by the ubiquitous disappearance of benthic foraminifers, suggestive of bottom water conditions unsuitable for life.

Post-Depositional Processes

Pronounced overprinting of the primary depositional signals by diagenetic processes occurs at all sites drilled on Leg 127. The most widespread process affecting the sediments is the alteration of opaline diatomaceous sediments to hard porcellanites and siliceous claystones with depth. Two silica transformations accompany the lithologic changes, opal-A to opal-CT and opal-CT to quartz. The opal-A/opal-CT transition is the most conspicuous change, as it affects all physical properties of the sediments as well as the interstitial water chemistry; this transition also is manifested in the downhole logs and in all seismic reflection records surrounding the sites as a strong bottom-simulating reflector which locally cuts across reflectors originating from stratal boundaries. The opal-A/opal-CT transition occurs at about 215 mbsf at Site 796 and at approximately 300 mbsf at Sites 794, 795, and 797, corresponding to present subsurface temperatures in the range of 36°–43°C. Opal-CT transforms to quartz about 80–150 m below the opal-A/opal-CT transition at all sites, corresponding to temperatures of 49°–62°C.

An additional significant post-depositional process influencing sediments in the Japan Sea is the biodegradation of organic matter. Organic matter preservation is rather low in the sedimentary section except for parts of the Quaternary at all sites and the upper Miocene at Sites 794 and 797 in the Yamato Basin. The degree of preservation and the pathways of degradation reflect supply, bottom water conditions during deposition, and rates of burial. The two sites in the Yamato Basin are characterized by interstitial waters with undepleted sulfate, low amounts of biogenic gas, and low to moderate rates of sedimentation. These trends are generally reversed at the Japan Basin sites, suggesting that sedimentation rates strongly influence the degradational processes affecting organic matter by controlling both the supply of material and the residence time of this material within the subsurface zones of bacterial decay.

These diagenetic transformations are both a hindrance and an aid to the geological interpretations. On the one hand, these processes severely limit our ability to see primary signals. The destruction of the siliceous microfossil record with burial is the best example of this condition. On the other hand, the diagenetic effects provide valuable information on the temperature history of the region. This aspect is extremely valuable at Site 796, where uplift may have caused recent perturbations of the heat flow. The benthic-free foraminifer assemblage is not caused by dissolution because planktonics which are more solution-susceptible than benthics are preserved.

REFERENCES

Abe, K., and Kanamori, H., 1970. Mantle structure beneath the Japan Sea as revealed by surface waves. *Tokyo Daigaku Jishin Kenkyusho Iho*, 48:1011–1021.

Amano, K., and Sata, H., 1989. Neogene tectonics of the central part of the northeast Honshu arc. *Chishitsugaka Ronshu*, 32:81–96.

Andrews, D. J., and Sleep, N. H., 1974. Numerical modelling of tectonic flow behind island arcs. *Geophys. J. R. Astron. Soc.*, 38:237-251.

Asano, K., Ingle, J. C., Jr., and Takayanagi, Y., 1969. Neogene planktonic foraminiferal sequence in northern Honshu. *In* Brönniman, R. P., and Renz, H. (Eds.), *Proc. 1st Int. Conf. Planktonic Microfossils*. Leiden (E. J. Brill), 1:14-25.

Barash, M. S., 1986. The paleoceanographic conditions of the formation of the late Miocene phosphatic horizon of the North Yamato Rise (Sea of Japan). *Oceanology*, 26:721-724.

Berggren, W. A., Kent, D. V., Flynn, J. J., and Van Couvering, J. A., 1985. Cenozoic geochronology. *Geol. Soc. Am. Bull.*, 96:1407-1418.

Boggs, S., Jr., 1984. Quaternary sedimentation in the Japan arc-trench system. *Geol. Soc. Am. Bull.*, 95:669-685.

Bukry, D., 1978. Biostratigraphy of Cenozoic marine sediment by calcareous nannofossils. *Micropaleontology*, 24:44-60.

Burckle, L. H., and Akiba, F., 1978. Implications of late Neogene freshwater sediment in the Sea of Japan. *Geology*, 6:123-127.

Canfield, D. E., and Berner, R. A., 1987. Dissolution and pyritization of magnetite in anoxic marine sediments. *Geochim. Cosmochim. Acta*, 51:645-659.

Celaya, M., and McCabe, R., 1987. Kinematic opening of the Sea of Japan and the bending of the Japanese islands. *Geology*, 15:53-57.

Chapman, M. C., and Solomon, S. C., 1976. North American plate boundary in northeast Asia. *J. Geophys. Res.*, 81:921-930.

Chase, C. G., 1978. Extension behind island arcs and motion relative to hot spots. *J. Geophys. Res.*, 83:5385-5387.

Chinzei, K., 1986. Opening of the Japan Sea and marine biogeography during the Miocene. *J. Geomagn. Geoelectr.*, 38:487-494.

Dewey, J. F., 1980. Episodicity, sequence and style at convergent plate boundaries. *In* Strangeway, D. (Ed.), *The Continental Crust and its Mineral Resources*. Geol. Assoc. Can., Spec. Rep., 20:553-574.

Dick, H.J.B., Marsh, N. G., and Bullen, T. D., 1980. Abyssal basalts from the Shikoku Basin: their petrology and major element geochemistry. *In* Klein, G. deV., Kobayashi, K., et al., *Init. Repts. DSDP*, 58: Washington (U.S. Govt. Printing Office), 843-872.

Donnelly, T. W., Melson, W., Kay, R., and Rogers, J.J.W., 1973. Basalts and dolerites of late Cretaceous age from the central Caribbean. *In* Edgar, N. T., Saunders, J. B., et al., *Init. Repts. DSDP*, 15: Washington (U.S. Govt. Printing Office), 989-1012.

Einsele, G., 1982. Mechanism of sill intrusion into soft sediment and expulsion of pore water. *In* Curray, J. R., Moore, D. G., et al., *Init. Repts. DSDP*, 64 (Pt. 2): Washington (U.S. Govt. Printing Agency), 1169-1176.

Froelich, P. N., Klinkhammer, G. P., Bender, M. L., Luedtke, N. A., Heath, G. R., Cullen, D., Dauphin, P., Hartman, B., Hammond, D., and Maynard, V., 1979. Early oxidation of organic matter in pelagic sediments of the eastern Equatorial Atlantic: suboxic diagenesis. *Geochim. Cosmochim. Acta*, 43:1075-1090.

Fujioka, K., 1986. Synthesis of Neogene explosive volcanism of the Tohoku arc, deduced from marine tephra drilled around the Japan Trench region, Deep Sea Drilling Project Legs 56, 57, and 87B. *In* Kagami, H., Karig, D. E., Coulbourn, W. C., et al., *Init. Repts. DSDP*, 87: Washington (U.S. Govt. Printing Office), 703-726.

Fukao, Y., and Furumoto, M., 1975. Mechanism of large earthquakes along the eastern margin of the Japan Sea. *Tectonophysics*, 25:247-266.

Gill, J., 1981. *Orogenic Andesites and Plate Tectonics*: New York (Springer-Verlag).

Gnibidenko, H., 1979. The tectonics of the Japan Sea. *Mar. Geol.*, 32: 71-87.

Hidaka, K., 1966. Japan Sea. *In* Fairbridge, R. (Ed.), *Encyclopedia of Oceanography*: New York (Reinhold), 417-424.

Hilde, T. W., and Wageman, J. M., 1973. Structure and origin of the Japan Sea. *In* Coleman, P. J. (Ed.), *The Western Pacific: Island Arcs, Marginal Seas, Geochemistry*: Perth (Univ. of Western Australia Press), 415-434.

Hirata, N., Kinoshita, H., Suyehiro, K., Suyemasu, M., Matsuda, N., Ouchi, T., Katao, H., Koresawa, S., and Nagumo, S., 1987. Report on the DELP 1985 cruises in the Japan Sea, Part II: seismic refraction experiment conducted in the Yamato Basin, southeast Japan Sea. *Tokyo Daigaku Jishin Kenkyusho Iho*, 62:347-365.

Hirata, N., Tokuyama, H., and Chung, T. W., 1989. An anomalously thick layering of the crust of the Yamato Basin, southeastern Japan Sea: the final stage of back-arc spreading. *Tectonophysics*, 165:303-314.

Iijima, A., Tada, R., and Watanabe, Y., 1988. Developments of Neogene sedimentary basins in the northeastern Honshu arc with emphasis on Miocene siliceous deposits. *J. Fac. Sci., Univ. Tokyo*, 21: 417-466.

Ingle, J. C., Jr., 1975a. Summary of late Paleogene and Neogene insular stratigraphy, paleobathymetry, and correlation, Philippine Sea and the Sea of Japan. *In* Karig, D. E., Ingle, J. C., Jr., et al., *Init. Repts. DSDP*, 31: Washington (U.S. Govt. Printing Office), 837-855.

Ingle, J. C., Jr., 1975b. Pleistocene and Pliocene foraminifera from the Sea of Japan. *In* Karig, D. E., Ingle, J. C., Jr., et al., *Init. Repts. DSDP*, 31: Washington (U.S. Govt. Printing Office), 693-702.

Ingle, J. C., Jr., 1981. Origin of Neogene diatomites around the North Pacific rim. *In* Garrison, R. S., Douglas, R., Pisciotto, K., Isaacs, C., and Ingle, J. C. (Eds.), *The Monterey Formation and Related Siliceous Rocks of California*. Soc. Econ. Paleontol. Mineral. Spec. Publ., 159-179.

Isezaki, N., 1986. A magnetic anomaly map of the Japan Sea. *J. Geomagn. Geoelectr.*, 38:403-410.

Jolivet, L., 1986. America-Eurasia plate boundary in eastern Asia and the opening of marginal basins. *Earth Planet. Sci. Lett.*, 81:282-288.

Jolivet, L., and Huchon, P., 1989. Crustal-scale strike-slip deformation in northern Japan. *J. Struct. Geol.*, 11:509-522.

Jolivet, L., Huchon, P., and Rangin, C., 1989. Tectonic setting of Western Pacific marginal basins. *Tectonophysics*, 160:23-47.

Kaneoka, I., 1986. Constraints on the time of the evolution of the Japan Sea based on radiometric ages. *J. Geomagn. Geoelec.*, 38:475-485.

Kaneoka, I., Notsu, K., Takigami, Y., Fujioka, K. and Sakai, H., in press. Constraints on the evolution of the Japan Sea based on ^{40}Ar-^{39}Ar ages and Sr isotopic ratios for volcanic rocks of Yamato Seamount chain in the Japan Sea. *Earth Planet. Sci. Lett.*

Karig, D. E., 1971. Origin and development of marginal basins in the western Pacific. *J. Geophys. Res.*, 76:2542-2561.

Karig, D. E., 1974. Evolution of arc systems in the western Pacific. *Annu. Rev. Earth Planet. Sci.*, 2:51-75.

Karig, D. E., Ingle, J. C., Jr., et al., 1975. *Init. Repts. DSDP*, 31: Washington (U.S. Govt. Printing Office).

Karlin, R., and Levi, S., 1983. Diagenesis of magnetic minerals in recent hemipelagic sediments. *Nature*, 303:327-330.

Karlin, R., and Levi, S., 1985. Geochemical and sedimentological control of the magnetic properties of hemipelagic sediments. *J. Geophys. Res.*, 90:10373-10392.

Katao, H., 1988. Seismic structure and formation of the Yamato Basin. *Tokyo Daigaku Jishin Kenkyusho Iho*, 63:51-86.

Kimura, G., Miyashita, S., and Miyasaka, S., 1983. Collision tectonics in Hokkaido and Sakhalin. *In* Hashimoto, M., and Uyeda, S. (Eds), *Accretion Tectonics in the Circum-Pacific Regions*: Tokyo (Terra Publ.), 69-88.

Kimura, G., and Tamaki, K., 1986. Collision, rotation and back-arc spreading in the region of the Okhotsk and Japan Seas. *Tectonics*, 5: 389-401.

Kobayashi, K., and Nomura, M., 1972. Iron sulfides in the sediment cores from the Sea of Japan and their geophysical implications. *Earth Planet. Sci. Lett.*, 16:200-208.

Kobayashi, Y., 1983. The initiation of the "subduction." *Earth Mon.*, 51:510-514.

Koizumi, I., 1979. The geological history of the Sea of Japan—based on sediments and microfossils. *Nihonkai (Japan Sea)*, 10:69-90.

Koizumi, I., 1983. Sedimentary environments of Neogene diatomaceous sediments, west coast of Japan. *In* Iijima, A., and Hein, J. (Eds.), *Siliceous Deposits in the Pacific Region*: Amsterdam (Elsevier), 347-360.

Koizumi, I., 1985. Diatom biochronology for late Cenozoic northwest Pacific. *Chishitsugaku Zasshi*, 91:195-211.

Koizumi, I., 1988. Early Miocene Proto-Japan Sea. *J. Paleontol. Soc. Korea*, 4:6-20.

Koizumi, I., and Tanimura, Y., 1985. Neogene diatom biostratigraphy of the middle latitude western North Pacific, Deep Sea Drilling Project Leg 86. *In* Heath, G. R., Burckle, L. H., et al., *Init. Repts. DSDP*, 86: Washington (U.S. Govt. Printing Office), 269-300.

Lallemand, S., and Jolivet, L., 1986. Japan Sea: a pull-apart basin? *Earth Planet. Sci. Lett.*, 76:375–389.

Ludwig, W. J., Murauchi, S., and Houtz, R. E., 1975. Sediments and structure of the Japan Sea. *Geol. Soc. Am. Bull.*, 86:651–664.

Matoba, Y., 1984. Paleoenvironment of the Sea of Japan. *In* Oertli, H. J. (Ed.), *Benthos'83: Proc. 2nd Int. Conf. Benthic Foraminifera*: 409–414.

Michael, P. J., and Chase, R. L., 1987. The influence of primary magma composition, H_2O and pressure on mid-ocean ridge basalt differentiation. *Contrib. Mineral. Petrol.*, 96:245–263.

Miyake, Y., Sugimura, Y., and Matsumoto, E., 1968. Ionium-thorium chronology of Japan Sea cores. *Rec. Oceanogr. Works Jpn.*, 9:189–195.

Miyashiro, A., 1986. Hot Regions and the origin of marginal basins in the western Pacific. *Tectonophysics*, 122:195–216.

Molnar, P., and Atwater, T., 1978. Inter-arc spreading and cordilleran tectonics as alternatives related to the age of subducted oceanic lithosphere. *Earth Planet. Sci. Lett.*, 41:330–340.

Nakamura, K., 1983. Possible nascent trench along the eastern Japan Sea as the convergent boundary between Eurasian and North American plates. *Tokyo Daigaku Jishin Kenkyusho Iho*, 58:711–722.

Okada, H., and Niitsuma, N., in press. *Phys. Earth Planet. Int.*

Otofuji, Y., and Matsuda, T., 1983. Paleomagnetic evidence for the clockwise rotation of southwest Japan. *Earth Planet. Sci. Lett.*, 62: 349–359.

Otofuji, Y., Hayashida, A., and Torii, M., 1985. When was the Japan Sea opened: Paleomagnetic evidence from southwest Japan. *In* Nasu, N., et al. (Eds.), *Formation of Active Ocean Margins*: Tokyo (Terra Publ.).

Otofuji, Y., Matsuda, T., and Nohda, S., 1985. Paleomagnetic evidence for the Miocene counterclockwise rotation of northeast Japan—rifting process of the Japan arc. *Earth Planet. Sci. Lett.*, 75:265–277.

Otsuki, K., 1989. Reconstruction of the Neogene tectonic stress field of NE Honshu arc from metalliferous veins. *Chishitsugaku Ronshu*, 32:281–304.

Pearce, J. A., Alabaster, T., Shelton, A. W., and Searle, M. P., 1981. The Oman ophiolite as a Cretaceous arc-basin complex: evidence and implications. *Philos. Trans. R. Soc. London*, A300:299–317.

Rahman, A., and Roth, P. H., 1989. Late Neogene calcareous nannofossil biostratigraphy of the Gulf of Aden region based on calcareous nannofossils. *Mar. Micropaleontol.*, 15:1–27.

Saunders, A. D., and Tarney, J., 1984. Geochemical characteristics of basaltic volcanism within back-arc basins. *In* Kokelaar, B. P., and Howells, M. F. (Eds.), *Marginal Basin Geology*: Oxford (Blackwell Scientific), 59–76.

Savostin, L. P., Zonenshain, L. A., and Baranov, B., 1983. Geology and plate tectonics of the Sea of Okhotsk. *In* Hilde, T. W., and Uyeda, S. (Eds.), *Geodynamics of the Western Pacific and Indonesian Regions.* Am. Geophys. Union Monogr., 11:343–354.

Seno, T., and Maruyama, S., 1984. Paleogeographic reconstruction and origin of the Philippine Sea. *Tectonophysics*, 102:53–84.

Sleep, N. H., and Toksöz, M. N., 1971. Evolution of marginal basins. *Nature*, 33:548–550.

Stoeser, D. B., 1975. Igneous rocks from Leg 30 of the Deep Sea Drilling Project. *In* Andrews, J. E., Packham, G., et al., *Init. Repts. DSDP*, 30: Washington (U.S. Govt. Printing Office), 401–414.

Sugi, N., Chinzei, K., and Uyeda, S., 1983. Vertical crustal movements of North-east Japan since middle Miocene. *In* Hilde, T.W., and Uyeda, S. (Eds.), *Geodynamics of the Western Pacific and Indonesian Regions.* Am. Geophys. Union Geodyn. Ser., 11:317–330.

Sun, S.-S., Nesbitt, R. W., and Sharuskin, A. Ya., 1979. Geochemical characteristics of mid-ocean ridge basalts. *Earth Planet Sci. Lett.*, 44:119–138.

Suzuki, U., 1979. Petroleum geology of the Sea of Japan, Northern Honshu. *Jpn. Assoc. Pet. Tech.*, 44:291–307.

Tada, R., Watanabe, Y., and Iijima, A., 1986. Accumulation of laminated and bioturbated Neogene siliceous deposits in Ajigaswa and Goshogawara areas, Aomori prefecture, northeast Japan. *J. Fac. Sci., Univ. Tokyo*, 21:139–167.

Takayasu, T., (Ed.), Matoba, Y., (Ed.), Haziota, K., et al., 1976. Guidebook for excursion 1, Oga Peninsula: *Int. Congr. Pacific Neogene Stratigr.*, Tokyo, Japan.

Tamaki, K., 1985. Two modes of back-arc spreading. *Geology*, 13:475–478.

Tamaki, K., 1986. Age estimation of the Japan Sea on the basis of stratigraphy, basement depth and heat flow data. *J. Geomagn. Geoelectr.*, 38:427–446.

Tamaki, K., 1988. Geological structure of the Sea of Japan and its tectonic implications. *Chishitsu Chosasho Geppo*, 39:269–365.

Tamaki, K., and Honza, E., 1985. Incipient subduction and obduction along the eastern margin of the Japan Sea. *Tectonophysics*, 119: 381–406.

Tamaki, K., and Kobayashi, K., 1988. Geomagnetic anomaly lineation in the Japan Sea. *Mar. Sci. Mon.*, 20:705–710.

Tapponier, P., Peltzer, G., LeDain, A. Y., Armijo, R., and Cobbold, P., 1982. Propagating extrusion tectonics in Asia: new insights from simple experiments with plasticine. *Geology*, 10:611–616.

Taylor, B., and Karner, G. D., 1983. On the evolution of marginal basins. *Rev. Geophys. Space Phys.*, 21:1727–1741.

Toksöz, M. N., and Bird, P., 1977. Formation and evolution of marginal basins and continental plateaus. *In* Talwani, M., and Pitman, W. C., III (Eds.), *Island Arcs, Deep Sea Trenches, and Backarc Basins.* Am. Geophys. Union, Maurice Ewing Ser., 1:379–393.

Toksöz, M. N., and Hsui, A. T., 1978. Numerical studies of back-arc convection and the formation of marginal basins. *Tectonophysics*, 50:177–196.

Tokuyama, H., Suyemasu, M., Tamaki, K., Nishiyama, E., Kuramoto, S., Suyehiro, K., Kinoshita, H., and Taira, A., 1987. Report on DELP 1985 cruises in the Japan Sea. Part III: seismic reflection studies in the Yamato Basin and the Yamato Rise area. *Tokyo Daigaku Jishin Kenkyusho Iho*, 62:367–390.

Tosha, T., and Hamano, Y., 1988. Paleomagnetism of Tertiary rocks from the Oga Peninsula and the rotation of northeast Japan. *Tectonics*, 7:653–662.

Tsuchi, R. (Ed.), 1981. *Neogene of Japan—Its Biostratigraphy and Chronology.* Shizuoka (Shizuoka Univ. Press).

Ujiie, H., and Ichikawa, M., 1973. Holocene to uppermost Pleistocene planktonic foraminifera in a piston core from the Sanin District, Sea of Japan. *Trans. Proc. Paleontol. Soc. Japan*, 91:137–150.

Uyeda, S., and Kanamori, H., 1979. Back-arc opening and the mode of subduction. *J. Geophys. Res.*, 84:1049–1062.

Vail, P. R., Mitchum, R. M., and Thompson, S., III, 1977. Seismic stratigraphy and global changes of sea level. Part 2: the depositional sequence as a basic unit for stratigraphic analysis. *In* Payton, C. E. (Ed), *Seismic Stratigraphy-Applications to Hydrocarbon Exploration*, AAPG Mem., 26:53–97.

Wu, F. T., 1978. Benioff zones, absolute motion and inter arc basins. *J. Phys. Earth.*, 26:539–554.

Zonenshain, L. P., and Savostin, L. A., 1981. Geodynamics of the Baikal rift zone and plate tectonics of Asia. *Tectonophysics*, 76:1–45.

Ms 127A-101